Bioorganic Chemistry 109 (2021) 104694

Contents lists available at ScienceDirect

Bioorganic Chemistry

journal homepage: www.elsevier.com/locate/bioorg

Design, synthesis and *in vitro* anticancer research of novel tetrandrine and fangchinoline derivatives

Xiu-zheng Gao [a,b,1], Xu-tao Lv [a,1], Rui-rui Zhang [b], Yang Luo [c], Mu-xuan Wang [a], Jia-shu Chen [a], Yu-kai Zhang [a], Bin Sun [a,*], Jin-yue Sun [b,*], Yu-fa Liu [a,*], Chao Liu [b,*]

[a] College of Chemistry, Chemical Engineering and Materials Science, Collaborative Innovation Center of Functionalized Probes for Chemical Imaging in Universities of Shandong, Key Laboratory of Molecular and Nano Probes, Ministry of Education, Shandong Provincial Key Laboratory of Clean Production of Fine Chemicals, Shandong Normal University, 88 East Wenhua Road, Jinan 250014, PR China

[b] Key Laboratory of Novel Food Resources Processing, Ministry of Agriculture and Rural Affairs/Key Laboratory of Agro-Products Processing Technology of Shandong Province/Institute of Agro-Food Science and Technology, Shandong Academy of Agricultural Sciences, 202 Gongye North Road, Jinan 250100, PR China

[c] Chongqing Academy of Chinese Materia Medica, Chongqing 400065, PR China

ARTICLE INFO

Keywords:
Fangchinoline derivatives
Tetrandrine derivatives
Anti-proliferative
Anti-migration
Apoptosis-inducing
PI3K/Akt/mTOR pathway

ABSTRACT

Cancer treatment is one of the major public health issues in the world. Tetrandrine (Tet) and fangchinoline (*d*-Tet) are two *bis*-benzyl isoquinoline alkaloids extracted from *Stephania tetrandra* S. Moore, and their antitumor activities have been confirmed. However, the effective dose of Tet and *d*-Tet were much higher than that of the positive control and failed to meet clinical standards. Therefore, in this study, as a continuation of our previous work to study and develop high-efficiency and low-toxic anti-tumor lead compounds, twenty new Tet and *d*-Tet derivatives were designed, synthesized and evaluated as antitumor agents against six cancer cell lines (H460, H520, HeLa, HepG-2, MCF-7, SW480 cell lines) and BEAS-2B normal cells by CCK-8 analysis. Ten derivatives showed better cytotoxic effects than the parent fangchinoline, of which **4g** showed the strongest cell growth inhibitory activity with an IC_{50} value of 0.59 μM against A549 cells. Subsequently, the antitumor mechanism of **4g** was studied by flow cytometry, Hoechst 33258, JC-1 staining, cell scratch, transwell migration, and Western blotting assays. These results showed that compound **4g** could inhibit A549 cell proliferation by arresting the G2/M cell cycle and inhibiting cell migration and invasion by reducing MMP-2 and MMP-9 expression. Meanwhile, **4g** could induce apoptosis of A549 cells through the intrinsic pathway regulated by mitochondria. In addition, compound **4g** inhibited the phosphorylation of PI3K, Akt and mTOR, suggesting a correlation between blocking the PI3K/Akt/mTOR pathway and the above antitumor activities. These results suggest that compound **4g** may be a future drug for the development of new potential drug candidates against lung cancer.

1. Introduction

Cancer is the world's major public health problem and is the first or second leading cause of death among people under the age of 70 in 91 of 172 countries according to World Health Organization (WHO) reports [1]. In 2018, there were approximately 18.1 million new cases of cancer worldwide, and 9.7 million patients died of cancer [2]. It is predicted that global cancer cases will increase to 19 million by 2025 and reach 24 million by 2035 [3]. The rapid growth of the cancer drug market is also driven by the continued growth of cancer incidence globally [4]. However, due to acquired resistance and multiple molecular types of cancer, there are fewer anticancer drugs currently available [5]. Scientists have studied many new antitumor drug candidates, but research is still underway [6,7]. Therefore, there is an urgent need to find novel, safe and effective antitumor drugs.

Stephaniae tetrandrae radix, a traditional Chinese medicine [8], is the dry root of *Stephania tetrandra* S. Moore (Fig. 1a), and its main medicinal monomer components are tetrandrine (Tet) and fangchinoline (*d*-Tet). It has been reported that Tet and *d*-Tet showed many pharmacological effects, such as anti-inflammatory [9,10], antitumor [11-15], anti-arrhythmia [16,17], antioxidation [18,19], anti-fibrosis [20], and multidrug resistance properties [21-24]. In particular, antitumor effects

* Corresponding authors.
E-mail addresses: sunbin_1978@sdnu.edu.cn (B. Sun), moon_s731@hotmail.com (J.-y. Sun), liuyufa@sdnu.edu.cn (Y.-f. Liu), liuchao555@126.com (C. Liu).
[1] These authors contributed equally to this work.

https://doi.org/10.1016/j.bioorg.2021.104694
Received 26 November 2020; Received in revised form 18 January 2021; Accepted 23 January 2021
Available online 4 February 2021

are considered the most obvious, and many scientists have conducted extensive studies on the antitumor effects of Tet, *d*-Tet and their derivatives. Previous studies have shown that Tet and *d*-Tet can induce tumor cell apoptosis through the death receptor pathway and the mitochondrial pathway [25]. Tet and *d*-Tet can upregulate the ratio of Fas/FasL, increase the expression of Bax and Bak proteins, reduce the expression of Bcl-2 protein, promote the release of cytochrome *c*, upregulate APAF-1, and activate Caspase-9 and Caspase-3 [26,27]. In addition, Tet and *d*-Tet can cause tumor cell autophagy by increasing the expression of the autophagy marker proteins LC3-II, GFP-LC3, *P*62 and Beclin1 in tumor cells [28-32]. Tet and *d*-Tet have also been reported to block the G1/S and G2/M tumor cell cycle to inhibit tumor cell proliferation.

Based on our previous research, Tet derivatives with benzyl bromide showed good inhibitory activity on HepG-2 tumor cells [33]. The introduction of fluorinated benzyl bromide into Tet could increase the inhibitory activity against A549 lung cancer cells while reducing the cytotoxicity for the human normal liver cell line HL-7702 [34]. Although these derivatives have great potential as anticancer agents, they also have limitations in clinical applications because of their low bioavailability and poor water solubility. Studies have shown that the introduction of sulfonyl can reduce the value of pKa, thereby increasing water solubility [35], enhancing biological activity [36], extending half-life and improving bioavailability [37]. Therefore, based on previous research, in this study, as a continuation of our previous work to study and develop high-efficiency and low-toxic anti-tumor lead compounds, 10 new Tet derivatives and 10 new *d*-Tet derivatives were designed and synthesized by introducing benzyl bromide containing halogen atoms and sulfonyl groups, respectively. The anticancer activities of all compounds were evaluated against A549, H460, H520, $HepG_2$, HeLa, and MCF-7 cells. The results showed that the anticancer activity of compound **4g** was significantly improved compared with that of the parent compound. Interestingly, compound **4g** has obvious selectivity for cancer cells because of its slight cytotoxicity to human normal lung epithelial cells BEAS-2B. Therefore, the anticancer molecular mechanism of compound **4g** was also studied in this paper.

2. Results and discussion

2.1. Chemistry

Tet and *d*-Tet are dibenzyl isoquinoline alkaloids and have been proven to have antitumor effects. However, their low activity limits their clinical application. Therefore, it is of great significance to modify the structure of Tet and *d*-Tet. Our research team proved that derivatives containing fluorine benzyl bromide groups could improve their antitumor activity. As the former work continues, this study plans to design and synthesize new derivatives and to identify those with better activity and lower toxicity as candidates in clinical applications.

The general preparation methods for the 10 new Tet derivatives and 10 new *d*-Tet derivatives are displayed in Scheme 1. The readily available starting material Tet was reacted with different benzyl bromides in DMF at 25 °C to 90 °C to give 10 double quaternary ammonium salt Tet derivatives **3a**-**3j**. In route b, Tet was demethylated in hydrobromic acid and glacial acetic acid at 90 °C to obtain *d*-Tet. *d*-Tet was then placed in DMF and treated with NaH at 0 °C for 2 h and stirred under argon protection to change into sodium phenolate (route c). The sodium phenolate was replaced by a different benzyl bromide to give *d*-Tet derivatives **4a-4c** (route d). Derivatives **4d-4j** were synthesized according to route e, and *d*-Tet was reacted with a series of sulfonyl chloride in dichloromethane at 0 °C using pyridine as an acid scavenger under argon protection. The progress of the chemical reaction was followed by TLC analyses, and all 20 new compounds were obtained with a yield of 51.5%-95.4%. All derivatives were characterized according to HR-MS, ^{1}H NMR and ^{13}C NMR spectra.

2.2. Biological evaluation

2.2.1. In vitro cytotoxicity assay

The antitumor effects of all derivatives were evaluated by the CCK-8 method against the H460, HeLa, A549, HepG-2, MCF-7 and H520 cell lines. Hydroxycamptothecin (HCPT) and the parent compound (Tet and *d*-Tet) were used as the reference standards. As shown in Table 1, the antitumor activities of all quaternary ammonium derivatives were decreased compared with that of tetrandrine, with IC_{50} values ranging from 19.65 to 60.23 μM, and compounds **4a**-**4c** showed similar antitumor activity to that of the parent compound (*d*-Tet). The most active derivatives were the sulfonyl analogs, and all 7 derivatives showed stronger antitumor activity against all the tested cells compared to that of the parent compound. Among them, compound **4g** was found to be the most potent against A549 cells with an IC_{50} value of 0.59 μM, which was 14.34-fold more active than *d*-Tet, 12.15-fold more active than Tet, and 2.12-fold more potent than HCPT. It is worth noting that the normal lung epithelial cell line BEAS-2B was less affected by cytotoxicity from compound **4g**, with an IC_{50} value of 16.07 μM, in comparison with the other tumor cell lines and with the purchased anticancer drug HCPT. These results showed that **4g** had a significant selectivity for the cancer cell lines, particularly for A549, and therefore, the A549 cell line was chosen for subsequent studies.

According to the cytotoxicity of all of the derivatives, the preliminary structure–activity relationship (SAR) can be evaluated. The introduction of the quaternary amine structure to Tet could not enhance its antitumor activity, possibly because the main antitumor active group of Tet was dibenzyl isoquinoline, and the introduction of the quaternary amine changed the polarity of the compound, which is consistent with previous reports [38]. The sulfonyl analogs expressed obviously enhanced antitumor activity relative to *d*-Tet in this study, and previous research has reported that the introduction of sulfonyl groups into drugs can increase their biological activity by increasing hydrogen bonding interactions [39]. In addition, the introduction of sulfonyl groups can reduce drug

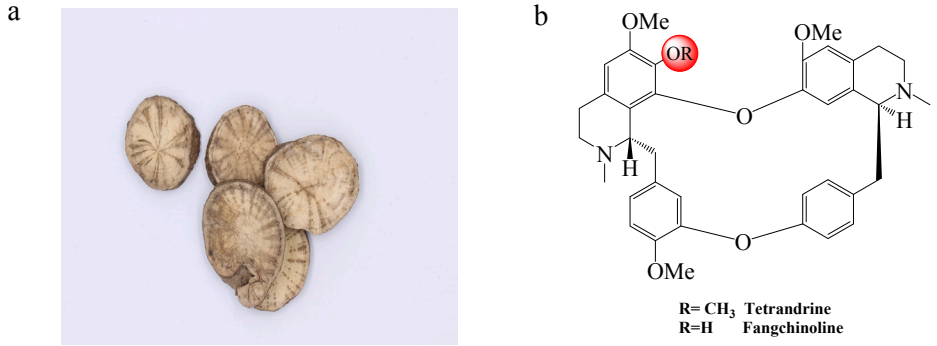

Fig. 1. (a) the root of *Stephania tetrandra* S. Moore; (b) the formula of tetrandrine and fangchinoline.

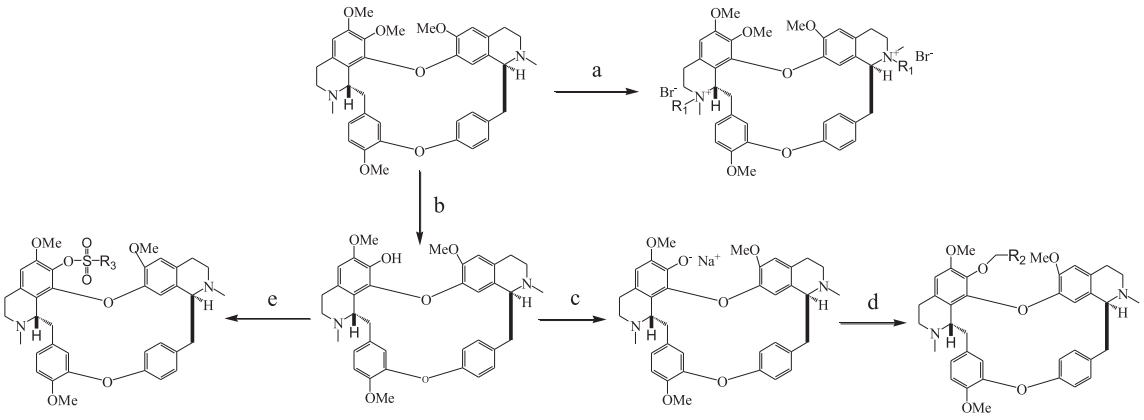

Scheme 1. Synthesis of tetrandrine and fangchinoline derivative. Reagents and conditions: (a) R_1 = CH_2X, Na_2CO_3, DMF, 25 °C − 90 °C; (b) 48% HBr solution, glacial acetic acid, 90 °C (c) NaH, N_2, DMF, 0 °C, 2 h (d) R_2 = CH_2X (e) pyridine, R_3 = SO_2Cl, 0 °C .

toxicity (**4g** is much less toxic to the normal lung epithelial cell line BEAS-2B). Moreover, the introduction of different lengths of alkyl groups on the sulfonyl group has little effect for the parent compound according to the anti-tumor activities of **4c-4e**. Jamieson *et al.* [37] summarized several common modification strategies to reduce the toxicity of drugs, such as introducing acidic groups, reducing basicity, and introducing polar groups to reduce lipophilicity and sulfonyl as a common polar group. The introduction of sulfonyl can reduce the lipophilicity of drug molecules and reduce toxicity. Among all sulfonyl derivatives, the compound activities in which the end of the substitution chain was connected with the benzene ring were obviously better than those of the alkyl compounds because of the conjugated structure formation between the sulfonyl group and the benzene ring structure, which makes the structure more stable [40]. The activity of **4h** is greater than that of **4i** shown that the introduction of different halogens on the benzene ring could impact activity, the possible reason may be that the electron absorption ability of fluorine is stronger, which makes the introduced structure more stable[15].

*2.2.1.1. Compound **4g** can inhibit A549 cell proliferation and arrest the cell cycle at G2/M phase.* Immortal proliferation and metastasis are among the main characteristics of cancer cells [41]. Cell cycle inhibitors have become an important means for treating cancer [42]. To assess the effect of compound **4g** on the growth of lung cancer A549 cells, a cell viability assay was designed using the CCK-8 assay. As shown in Fig. 2a, 4 g showed a remarkable anti-proliferative effect in a time- and concentration-dependent manner. The IC_{50} value of A549 cells treated with compound **4g** for 24 h was 1.317 μM, as shown in Fig. 2b. As the treatment time increased, the inhibition rate of the cells gradually increased. When A549 cells were treated with **4g** for 48 h, the IC_{50} value of compound **4g** in A549 cells was 0.68 μM, and for 72 h, it was 0.511 μM, as shown in Fig. 2c-d.

To further evaluate the antiproliferative effect of compound **4g**, a colony formation assay was designed. As shown in Fig. 2e, compound **4g** significantly inhibited the colony formation of A549 cells in a concentration-dependent manner. Moreover, compound **4g** can shrink the shape of A549 cells, as shown in Fig. 2f. Therefore, compound **4g** inhibited the proliferation of A549 cells.

To explore the mechanism of cell proliferation inhibition by compound **4g**, its effect on the distribution of A549 cells at various cell cycle stages was assessed by flow cytometry. As shown in Fig. 3a–b, after treatment of A549 cells with 1 μM, 2 μM, and 3 μM **4g**, there was a significant amount of dose-dependent accumulation at the G2/M phase. The percentage of the G_2/M phase increased from 7.43% to 10.81%, 15.51% and 19.48%, respectively. These results clearly indicate that compound **4g** can arrest the cell cycle at the G2/M phase in a dose-dependent manner in A549 cells. In addition, the expression of cell cycle factor-related proteins in A549 cells was analyzed. A549 cells were treated with different concentrations of **4g** for 48 h, and the protein levels of cyclins such as cyclinB1, CDK1 and *P*21 were examined. As a result, as shown in Fig. 3c-d, the protein levels of cyclin B1 and CDK1 were significantly decreased after **4g** treatment, and the protein level expression of *P*21 was significantly increased in a concentration-dependent manner. These results suggest that **4g** may arrest the G_2/M cell phase in A549 cells through downregulation of cyclin B1 and CDK1 and upregulation of *P*21.

*2.2.2. Compound **4 g** inhibits A549 cell migration and invasion*

To investigate whether **4 g** can influence A549 cell migration and invasion, wound healing and transwell assays were carried out. The results are shown in Figs. 4-5. Cell migration was significantly inhibited with increasing **4g** concentration, and the migration distance of A549 cells was decreased from 149 ± 5.41 to 25.43 ± 1.34 (Fig. 4a-c). The transwell assay was also performed after compound **4g** treatment, and the results showed that **4g** inhibited cell migration in a dose-dependent manner (Fig. 5). The number of migrated and invasive A549 cells was decreased from 100% to 10 ± 4.33% and 100% to 13 ± 3.18%, respectively. All of the results showed that compound **4g** can inhibit the migration of A549 cells.

According to reports, MMPs play an important role in the invasion and metastasis of cancer cells by degrading the ECM, and high levels of MMP-2 and MMP-9 expression are associated with poor prognosis of cancer [43]. To further verify the results, MMP-2 and MMP-9 proteins were detected using Western blot analysis in this study. As shown in Fig. 6, the expression levels of MMP-2 and MMP-9 showed a dose-dependent decrease. These results indicated that compound **4g** may inhibit invasion and migration by inhibiting the expression of MMP-2 and MMP-9 in A549 cells.

*2.2.3. Compound **4g** induced apoptosis in A549 cells*

Apoptosis is a basic biological phenomenon of cells and plays a key role in the removal of unwanted or abnormal cells in multicellular organisms. To assess whether **4g** can induce apoptosis in A549 cells, Annexin V-FITC/PI double staining was carried out to measure the population of apoptotic cells. As shown in Fig. 7a-b, the results of annexin V-FITC/PI indicated that **4g** triggered apoptosis of A549 cells, and the percentage of apoptotic cells increased from 9.48% (0 μM) to 13.13% (1 μM), 21.33% (2 μM), and 41.00% (3 μM), respectively. Hoechst 33,258 is a nuclear dye commonly used to detect apoptosis. In this study, A549 cells were treated with **4g** for 48 h, stained with Hoechst 33258, and visualized by confocal laser scanning microscopy. Based on the results (Fig. 7c), the number of bright blue cells increased significantly and showed typical apoptotic characteristics, cell shrinkage and chromatin condensation as the **4g** concentration increased.

Table 1
Cytotoxicity of 21 derivatives to 7 cell lines.

Compounds	Substitutent		IC50 (μM)						
	R1/R2/R3	X	A549	H520	HepG-2	MCF-7	Hela	H460	BASE-2S
3a	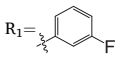	Br	30.12	46.80	58.54	53.08	36.02	47.75	30.43
3b		Br	36.07	41.08	60.23	44.07	40.65	37.06	43.91
3c		Br	25.96	30.54	25.04	38.56	39.41	42.65	42.12
3d		Br	29.54	26.44	28.035	31.43	36.85	41.84	36.91
3e	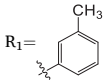	Br	30.59	46.58	37.02	43.73	30.90	47.53	33.02
3f	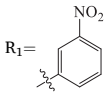	Br	37.45	50.65	32.04	46.84	48.94	50.02	41.42
3g		Br	46.35	49.56	58.01	37.28	49.87	43.90	48.33
3h	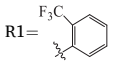	Br	19.65	21.034	25.51	37.85	24.52	26.10	33.91
3i	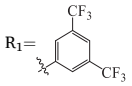	Br	30.56	34.83	36.87	39.04	38.04	36.87	41.04
3j	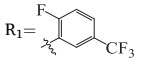	Br	39.02	57.33	51.30	46.79	46.52	40.33	50.42
4a	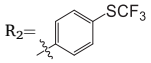		6.009	3.47	3.26	4.60	7.23	5.28	11.72
4b	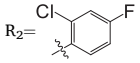		7.67	6.48	5.89	7.04	8.65	7.38	17.042
4c	$R_3 = CH_3$		6.63	6.54	6.892	7.26	6.124	6.31	11.03
4d	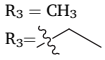		5.05	6.86	3.564	4.55	6.51	4.56	16.26
4e	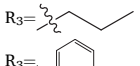		5.23	6.25	4.41	2.71	5.87	4.45	18.04
4f	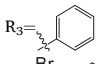		0.98	1.72	2.67	4.80	2.59	2.92	12.04
4g	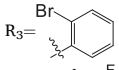		0.59	1.34	2.09	2.73	2.39	1.03	16.07
4h	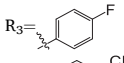		1.156	2.68	4.49	4.47	6.58	1.75	14.56
4i	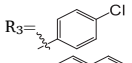		2.44	3.47	4.71	4.39	4.00	2.45	14.03
4j	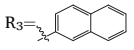		1.01	1.87	0.83	3.44	3.07	1.27	16.06
TET			6.97	7.32	7.27	8.76	15.43	8.32	10.03
DTET			7.46	8.34	9.03	11.2	11.54	8.23	9.98
HCPT			1.06	2.34	1.13	1.75	1.87	2.11	17.65

(Result of CCK-8 assay after 48 h drug treatment; the values are average for at least 3 independent experiments; variation ± 10%).

Mitochondria play an important role in regulating apoptosis. Mitochondrial membrane potential collapse is an early feature of apoptosis. Fluorescent probe JC-1 staining was used to evaluate changes in mitochondrial membrane potential by confocal microscopy. The fluorescence of the mitochondrial membrane potential of normal cells stained with JC-1 dye was red (JC-1 aggregate), while the mitochondrial membrane potential of apoptotic cells was green (JC-1 monomer). As a result, as shown in Fig. 8, as the concentration of **4g**-treated cells increased, the green fluorescence gradually increased, and the red fluorescence gradually decreased, indicating that the mitochondrial membrane potential gradually decreased. These results suggested that **4g** could induce A549 cell apoptosis by decreasing the mitochondrial membrane potential in a dose-dependent manner.

Apoptosis signaling is regulated by many apoptosis-related proteins, including Bcl-2, Bax, cleaved caspase-3, cleaved caspase-9 and cytochrome *c*. In this study, the expression levels of apoptosis-related proteins were analyzed by Western blot assay. The results are shown in Fig. 9. The expression level of the anti-apoptotic protein Bcl-2 was decreased, while the expression level of the pro-apoptotic protein Bax was increased, after treatment with 1, 2, and 3 μM **4g**, compared to that for control cells. In addition, after treatment of A549 cells with **4g**, cleaved caspase-3, cleaved caspase-9 and cytochrome *c* were significantly increased. The above results revealed that **4g** can induce A549 cell apoptosis through the intrinsic pathway regulated by mitochondria.

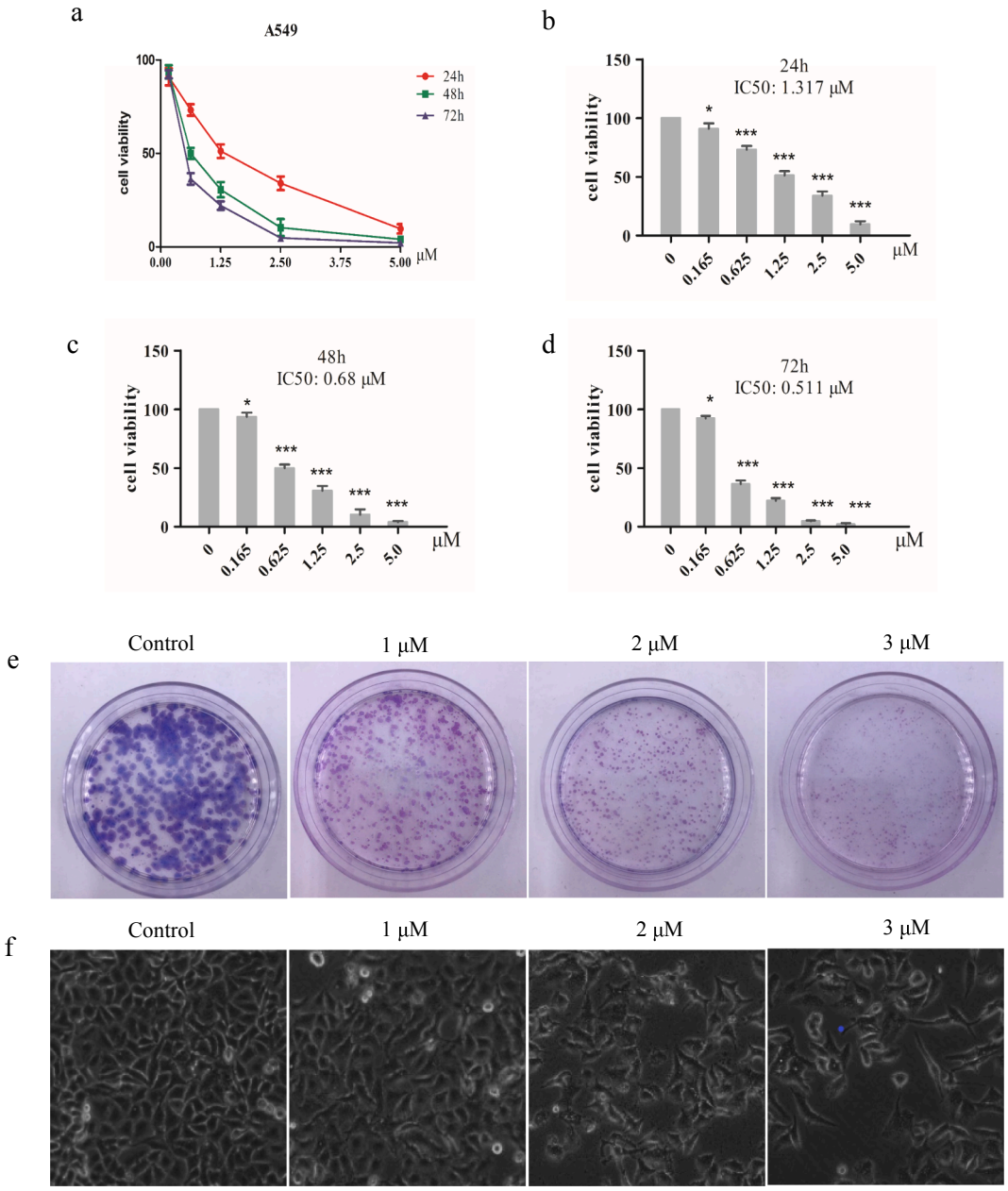

Fig. 2. Effect of compound 4 g on cell viability and cell growth. (a-d) A549 cells were treated with different concentrations of compound 4 g (0, 0.165, 0.625, 1.25, 2.5, 5 μM) for 24 h, 48 h, 72 h, and IC_{50} was measured using Graphpad prism software. Cell viability was measured by the CCK-8 assay. Colony formation test A549 cells were exposed to compound 4 g at the indicated concentrations. The number of colony formation was shown by Giemsa staining. (e) Changes in cell morphology of A549 cells treated with compound 4 g (0, 1, 2, 3 μM) at different concentrations for 48 h were photographed using a fluorescence microscope. (f) Using a fluorescent inverted microscope 100x to capture the changes in cell morphology of A549 cells treated with compound 4 g (0, 1, 2, 3 μM) at different concentrations for 48 h. * $P < 0.05$, ** $P < 0.01$, *** $P < 0.001$.

*2.2.4. Compound **4g** inhibits the PI3K/Akt/mTOR signaling pathway in A549 cells*

The PI3K/Akt/mTOR signaling pathway plays an important role in cell growth, proliferation, apoptosis, etc. PI3K activates the downstream serine/threonine kinase Akt, which in turn, through a cascade of regulators, triggers the phosphorylation and activation of the serine/threonine kinase mTOR [44]. PI3K/Akt/mTOR, a major intracellular signaling pathway, has received much attention in recent years given its potential role in cancer [45]. Dangelo *et al.* [46] found that after introducing fluoro benzene sulfonyl into the mother nucleus, compounds have strong inhibitory activity against both PI3K and mTOR. This study also investigated the effect of compound **4 g** on the PI3K/Akt/mTOR signaling pathway in A549 cells. The results are shown in Fig. 10. The levels of PI3K, Akt and mTOR did not change significantly in 4**g**-treated A549 cells, while the expression of p-PI3K, p-AKT, and p-mTOR in **4g**-treated A549 cells was significantly decreased, and the expression level of PTEN was increased in A549 cells in a dose-dependent manner. Thus, these data suggested that compound **4g** inhibited the activation of the PI3K/Akt/mTOR signaling pathway.

3. Conclusion

In summary, 10 tetrandrine and 10 fangchinoline derivatives were designed and synthesized, and the *in vitro* antitumor activities of these compounds against six cancer cell lines and normal lung epithelial BESA-2B cells were assessed by CCK-8 analysis. The results indicated

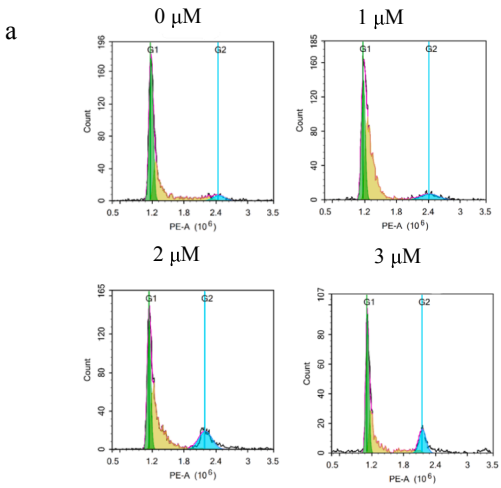

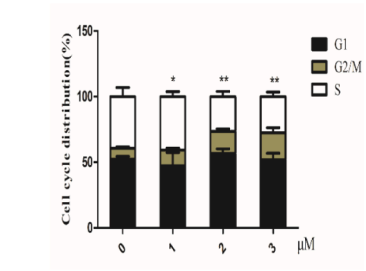

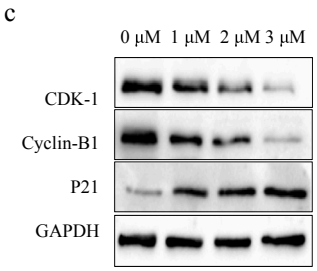

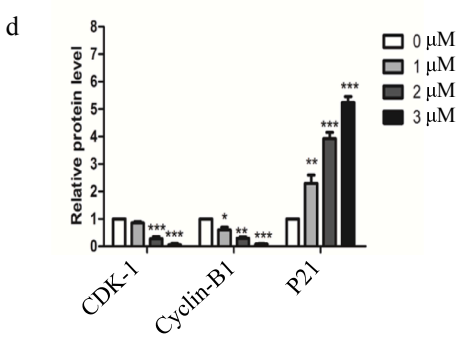

Fig. 3. Compound 4 g triggers cell cycle arrest in A549 cells. (a-b) Flow cytometry analysis showed the distribution of cells treated with 4 g at 0, 1, 2, 3 μM at different stages of the cell cycle. (c) Western blotting shows that compound 4 g is effective against CDK-1, Cyclin-B1 in A549 cells and *P*21 protein expression. The experiment was performed 3 times. (d) Measure the gray value of Western blot using Graphpad prism software. The result is the average of 3 replicates ± SD. * $P < 0.05$, ** $P < 0.01$, *** $P < 0.001$.

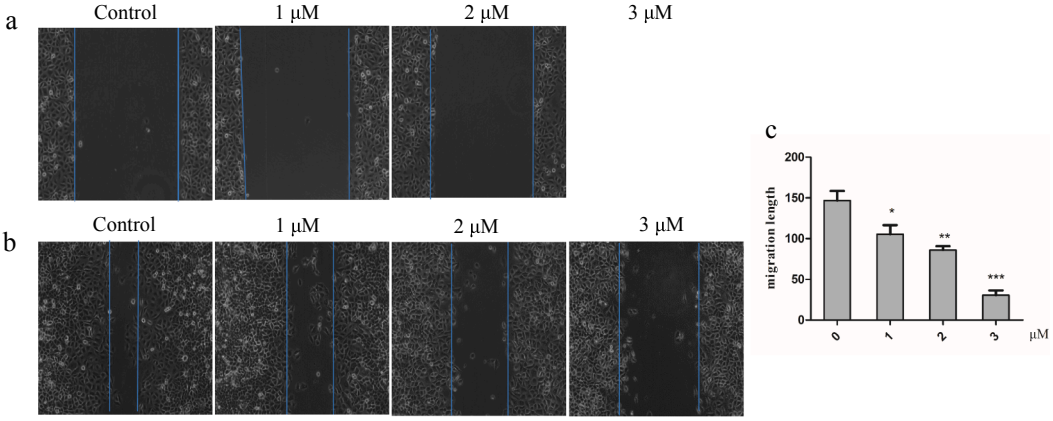

Fig. 4. Effect of Compound 4 g on cell migration. (a) A549 cells of the same wound were treated with different concentrations of compound 4 g (0, 1, 2, 3 μM) for 48 h the changes of the wound were photographed using a fluorescent inverted microscope. (b) A549 cells of the same width wound were treated with different concentrations of compound 4 g (0, 1, 2, 3 μM) for 48 h and the changes of the wound were photographed using a fluorescent inverted microscope. (c) Migration distance measured using Graphpad prism software. *P < 0.05, **P < 0.01, ***P < 0.001.

that the antitumor activities of the sulfonyl fangchinoline derivatives are significantly higher than that of the fangchinoline base. Among them, compound **4g** was found to be the most potent against A549 cells, with an IC_{50} value of 0.59 μM, which was 2.12-fold more active than the clinically commonly used anticancer drug HCPT. Compound **4g** inhibited A549 cell proliferation by arresting the cell cycle at the G2/M phase and inhibiting cell migration and invasion by reducing MMP-2 and MMP-9 expression. Moreover, compound **4g** is capable of triggering mitochondria-mediated intrinsic pathways to induce apoptosis and exert antitumor effects by modulating the PI3K/Akt/mTOR signaling pathway. Our current results indicate that **4g** is a potential candidate for the development of novel anti-human lung cancer cells.

4. Experimental section

4.1. Chemistry

4.1.1. General

Tet and *d*-Tet were extracted from Stephaniae tetrandrae radix according to our previous research [47]. *Stephaniae tetrandrae* S. Moore was purchased from a Chinese medicine store and was identified by Prof Chenggang Shan, Institute of Agro-Food Science and Technology,

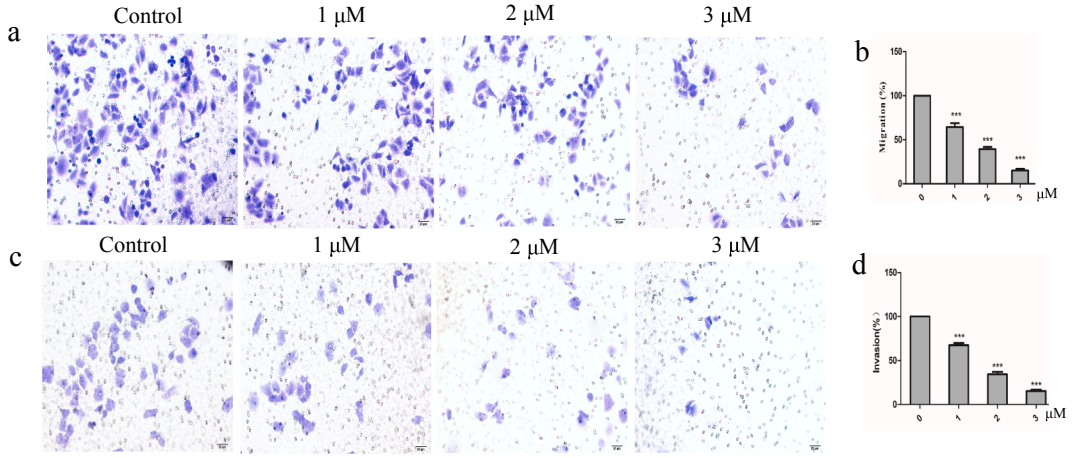

Fig. 5. Cell migration and cell invasion transwell assay. (a) Effect of compound 4 g on cell migration. A549 cells in the upper chamber of transwell chamber with different concentrations of compound 4 g (0, 1, 2, 3 μM) (lower chamber 10% serum-containing medium) were stained with Giemsa dye, and the migration of the chamber was photographed with a microscope. (c) Effect of compound 4 g on cell invasion. Add diluted Matrigel to the bottom of the upper chamber of the transwell chamber, incubate for 4–5 h to dry it into a gel, and use different concentrations of compound 4 g (0, 1, 2, 3 μM) A549 cells in the upper chamber of the transwell chamber 24 h. After 1 h (in the lower chamber, 10% serum-containing medium), stain the cells with Giemsa dye and use a microscope to photograph the invasion of the chamber. (b) (d) the number of migration and invasion cells. Measurements were performed using Graphpad prism software. *P < 0.05 , **P < 0.01, ***P < 0.001.

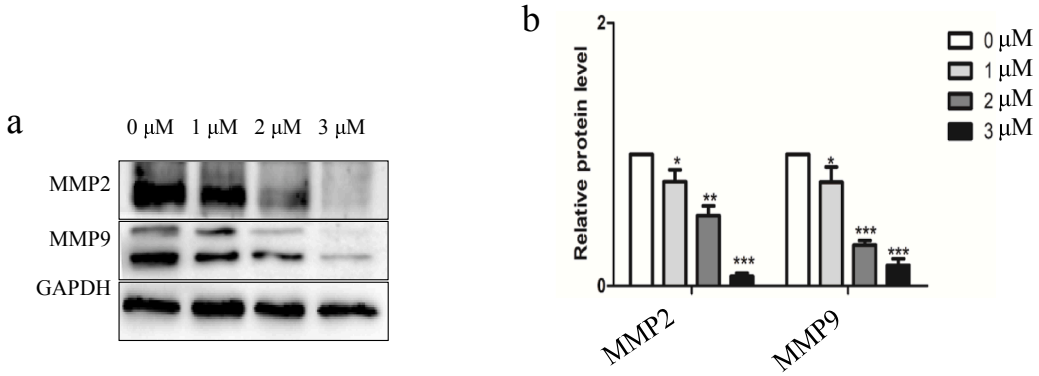

Fig. 6. Compound 4 g affects the expression of MMP-2 and MMP-9. (a) Western blot showed that compound 4 g had an effect on MMP2 and MMP9 protein expression in A549 cells. The experiment was performed 3 times. (b) Western blot gray values were measured using Graphpad prism software. *P < 0.05, **P < 0.01, ***P < 0.001.

Shandong Academy of Agriculture Sciences (IAFST, SAAS), Jinan, China. A voucher specimen (No. 18–08-79) (Fig. 1a) was deposited at the laboratory of Bioactive Substances and Functional Foods, IAFST, SAAS. The progress of the reaction was monitored by thin layer chromatography on silica gel GF-254. Separation and purification were performed by column chromatography using silica gel (Qingdao 200–300 mesh). ^{1}H NMR and ^{13}C NMR spectra were obtained using a Bruker AV400 spectrometer in $CDCl_3$ or CD_3OD with tetramethylsilane as an internal standard. HRMS data were obtained using a UHR-TOF-MS instrument (Bruke).

4.1.2. Synthesis of tetrandrine derivatives

A mixture of tetrandrine (100 mg, 0.16 mM) and Na_2CO_3 (34 mg, 0.32 mM) was dissolved in DMF, R_1CH_2X (0.32 mM) was slowly added dropwise at 25 °C to 90 °C with stirring, and the reaction was completed by TLC analysis. The solution was cooled to room temperature and evaporated by rotary evaporation using an oil pump. The residue was purified by column chromatography, and **3a-3j** was obtained by using CH_2Cl_2/CH_3OH as the eluent.

3a N,N'-di(m-F-Benzyl) Tet, ammonium dibromide as a white powder, ^{1}H NMR (400 MHz, CD_3OD) δ 7.43 (dd, J = 17.0, 9.5 Hz, 3H), 7.33 (t, J = 7.5 Hz, 4H), 7.16 (s, 1H), 7.15 (s, 2H), 7.13 (s, 1H), 7.11 (s, 1H), 7.09 (s, 1H), 7.07 (s, 1H), 7.05 (s, 1H), 6.94 (dd, J = 18.5, 8.3 Hz, 2H), 6.79 (d, J = 14.1 Hz, 2H), 6.69 (d, J = 7.6 Hz, 1H), 6.56 (s, 1H), 6.20 (s, 1H), 5.13 (d, J = 9.1 Hz, 1H), 4.94 (d, J = 5.9 Hz, 1H), 4.80 (s, 2H), 4.57 (d, J = 17.0 Hz, 6H), 3.78 (dd, J = 34.4, 4.5 Hz, 9H), 3.67–3.39 (m, 12H), 3.30 (s, 4H), 2.75 (s, 3H). ^{13}C NMR (101 MHz, CD_3OD) δ 153.84, 149.95, 149.67, 148.59, 146.38, 143.99, 138.70, 134.87, 134.55, 133.73, 133.69, 132.61, 132.61, 132.03, 131.82, 131.27, 131.24, 131.10, 130.68, 130.60, 125.51, 125.37, 124.90, 124.50, 124.47, 123.68, 122.20, 121.49, 120.96, 115.84, 115.47, 115.26, 114.18, 112.78, 112.52, 106.79, 69.44, 67.61, 67.02, 59.94, 58.52, 57.45, 57.06, 55.57, 55.24, 53.72, 49.75, 39.33, 36.32, 25.47, 23.26, 19.50; HRMS (ESI): calcd for $C_{52}H_{54}F_2N_2O_6^{2+}$ m/z: 420.1969, found: 420.1959, Yield: 89%.

3b N, N'-di(m-Cl-benzyl)-Tet ammonium dibromide as a white powder. ^{1}H NMR (400 MHz, CD_3OD) δ 7.65 (d, J = 13.8 Hz, 2H), 7.61–7.47 (m, 5H), 7.42 (t, J = 7.9 Hz, 2H), 7.15 (s, 1H), 7.03 (d, J = 8.2 Hz, 1H), 6.94 (d, J = 8.4 Hz, 1H), 6.88 (dd, J = 8.3, 2.4 Hz, 1H), 6.78 (dd, J = 9.4, 3.6 Hz, 2H), 6.60 (dd, J = 8.2, 1.8 Hz, 1H), 6.48 (s, 1H), 6.12 (s, 1H), 5.04 (d, J = 9.7 Hz, 2H), 4.77–4.54 (m, 8H), 4.49–4.35 (m, 2H), 3.91 (dd, J = 17.8, 4.1 Hz, 2H), 3.87–3.80 (m, 6H), 3.63 (s, 3H), 3.56 (d, J = 9.5 Hz, 2H), 3.43 (s, 3H), 3.29 (d, J = 7.0 Hz, 3H), 3.20 (dd, J = 16.2, 8.2 Hz, 2H), 2.65 (s, 3H); ^{13}C NMR (101 MHz, CD_3OD) δ

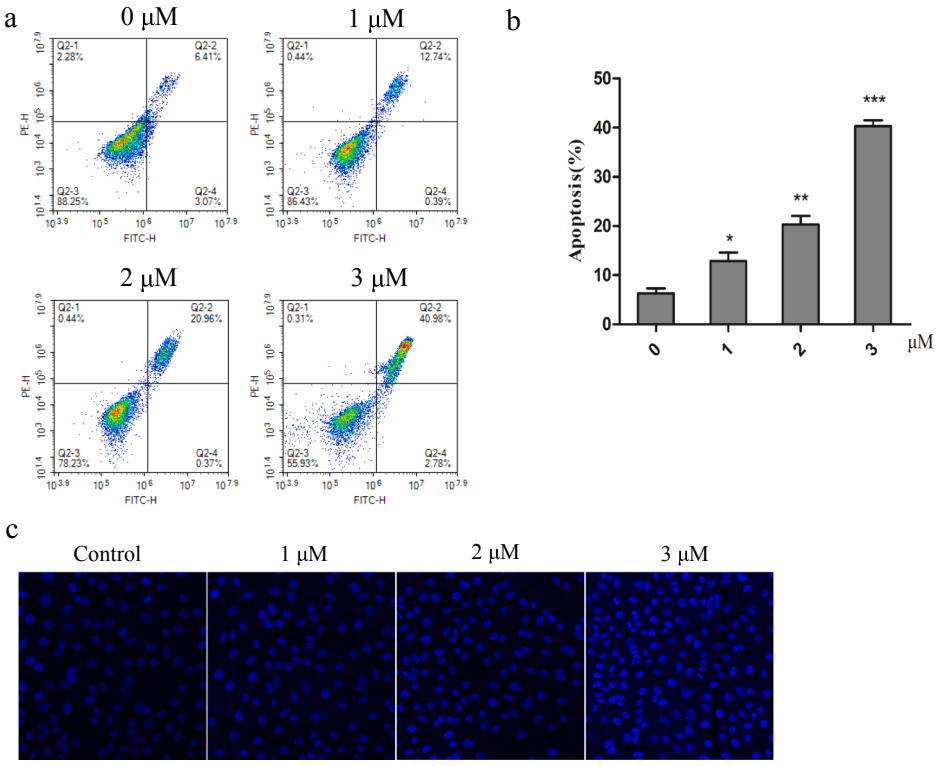

Fig. 7. Compound 4 g induce apoptosis of A549 cells. (a) Apoptosis analysis of A549 cells treated with different concentrations compound 4 g by flow cytometry. (b) The percentage of apoptotic cells was quantified by Graphpad software. Statistical results were represented as mean ± SD of three independent experiments. *P < 0.05, **P < 0.01, ***P < 0.001. (c) Hoechst33258 staining was used to show the compound 4 g induced morphological cellular changes.

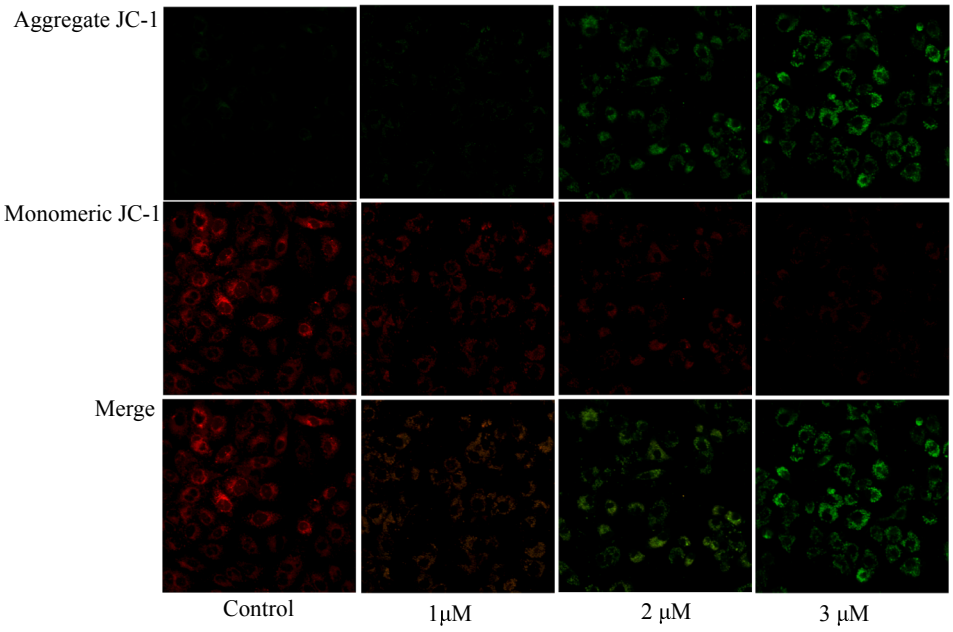

Fig. 8. Compound 4 g reduce mitochondrial membrane potential of A549 cells. A549 cells were treated with 0, 1, 2, 3 μM compound 4 g for 48 h. Mitochondrial membrane potential was assessed after staining with JC-1 dye .

154.90, 153.80, 150.03, 149.84, 148.60, 146.32, 144.09, 138.54, 134.95, 134.56, 132.63, 132.55, 131.94, 131.87, 131.68, 131.57, 131.10, 131.07, 130.90, 130.78, 130.68, 130.62, 129.59, 129.29, 128.53, 125.61, 124.25, 123.58, 121.71, 121.19, 120.39, 115.23, 113.98, 112.81, 112.46, 106.62, 68.72, 65.76, 63.60, 59.86, 55.30, 55.23, 54.88, 54.55, 53.64, 50.26, 39.17, 36.04, 23.19, 23.10; HRMS (ESI): calcd for $C_{52}H_{54}Cl_2N_2O_6^{2+}$ *m/z*: 436.1674, found: 436.1629. Yield: 85.3%.

3c N, N'-di(m-Br-benzyl)-Tet ammonium dibromide as a white powder. ^{1}H NMR (400 MHz, CD_3OD) δ 7.80 (d, J = 8.8 Hz, 2H), 7.73 (dd, J = 14.5, 7.3 Hz, 2H), 7.59 (d, J = 7.6 Hz, 1H), 7.53–7.41 (m, 3H), 7.35 (t, J = 7.9 Hz, 1H), 7.15 (s, 1H), 7.05–6.78 (m, 6H), 6.69–6.61 (m, 1H), 6.51 (s, 1H), 6.13 (s, 1H), 5.02 (t, J = 9.6 Hz, 2H), 4.74–4.35 (m, 8H), 3.84 (d, J = 3.6 Hz, 6H), 3.65 (s, 3H), 3.61–3.47 (m, 4H), 3.43 (s, 3H),

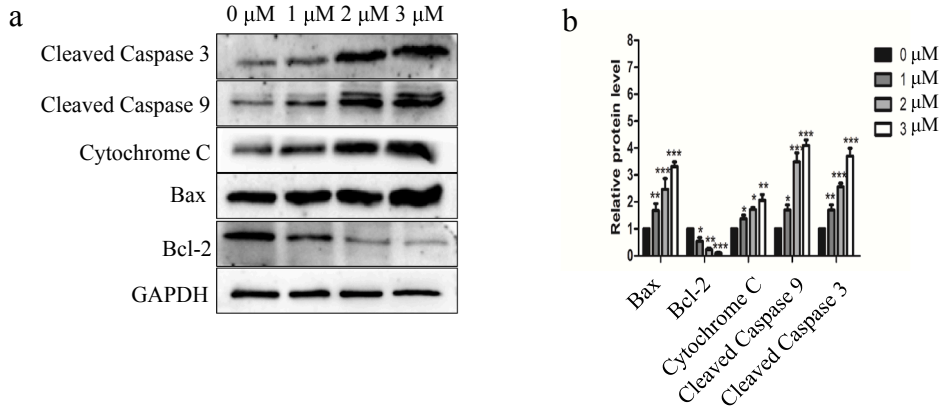

Fig. 9. Compound 4 g induces apoptosis in the mitochondrial pathway in A549 cells. (a) Western blot shows that compound 4 g is effective for mitochondrial pathway protein expression in A549 cells. (b) Measure the gray value of Western blot using Graphpad prism software. The result is the mean ± SD of 3 replicates. * $P < 0.05$, ** $P < 0.01$, *** $P < 0.001$.

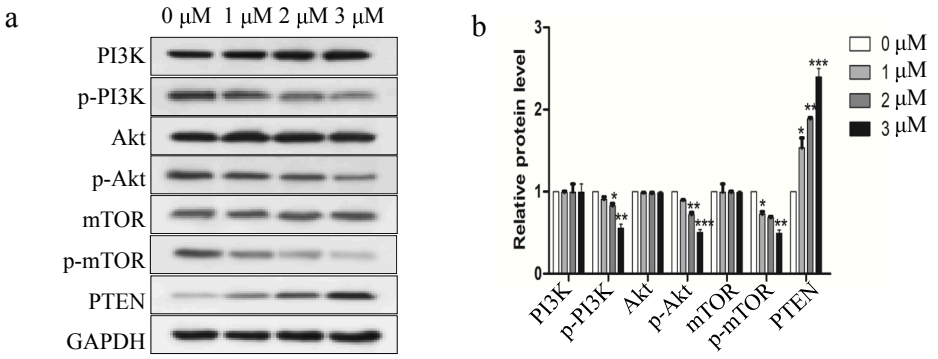

Fig. 10. Compound **4 g** induces apoptosis through the PI3K/Akt/mTOR signaling pathway. (a) P13K, p-PI3K, Akt, p-Akt, mTOR, p-mTOR and PTEN expression levels in A549 cells treated with **4 g** (0, 1, 2, 3 μM, 48 h) were verified by western blotting. (b) Measure the gray value of Western blot using Graphpad prism software. The result is the mean ± SD of 3 replicates. * $P < 0.05$, ** $P < 0.01$, *** $P < 0.001$.

3.30 (s, 3H), 3.20 (dd, $J = 19.6$, 8.1 Hz, 2H), 3.06–2.88 (m, 2H), 2.65 (s, 3H); ^{13}C NMR (101 MHz, CD_3OD) δ 154.94, 153.83, 150.07, 149.90, 148.66, 146.35, 144.15, 138.55, 135.44, 134.73, 133.89, 133.73, 132.83, 132.14, 131.82, 131.49, 131.07, 130.96, 130.80, 129.85, 129.55, 128.51, 125.60, 124.18, 123.56, 122.91, 122.51, 122.45, 121.66, 121.12, 120.45, 115.26, 114.04, 112.86, 112.44, 106.58, 68.62, 65.86, 63.55, 59.86, 55.30, 55.23, 54.88, 54.55 53.64, 50.26, 39.17, 36.04, 23.19, 23.10; HRMS (ESI): calcd for $C_{52}H_{54}Br_2N_2O_6^{2+}$ *m/z*: 481.1159, found: 481.1180. Yield: 78.6%.

3d N, N'-di(o-I-benzyl)-Tet ammonium dibromide as a white powder. ^{1}H NMR (400 MHz, CD_3OD) δ 7.89 (dd, $J = 16.8$, 8.2 Hz, 4H), 7.55 (d, $J = 7.6$ Hz, 1H), 7.44 (d, $J = 6.3$ Hz, 2H), 7.25 (t, $J = 7.8$ Hz, 1H), 7.14 (dd, $J = 17.4$, 9.5 Hz, 2H), 6.88 (ddd, $J = 17.1$, 14.2, 8.9 Hz, 4H), 6.74 (s, 1H), 6.69 (d, $J = 8.1$ Hz, 1H), 6.49 (s, 1H), 6.08 (s, 1H), 4.97 (d, $J = 9.6$ Hz, 2H), 4.62 (d, $J = 13.2$ Hz, 2H), 4.51 (d, $J = 5.9$ Hz, 2H), 4.36 (s, 1H), 3.83 (s, 2H), 3.80 (s, 5H), 3.62 (d, $J = 6.6$ Hz, 3H), 3.59–3.41 (m, 7H), 3.36 (s, 3H), 3.26 (s, 2H), 3.25 (d, $J = 3.2$ Hz, 3H), 3.23–3.09 (m, 2H), 2.60 (s, 3H); ^{13}C NMR (101 MHz, CD_3OD) δ 154.93, 153.85, 150.02, 149.94, 148.70, 146.39, 144.22, 141.29, 140.46, 139.93, 138.52 , 133.17, 132.57, 131.87, 131.73, 131.35, 131,14, 131.00, 130.85, 130.67, 129.75, 129.41, 128.56, 125.57, 124.09, 123.54, 122.74, 121.58, 121.08, 120.50, 117.64, 115.34, 114.07, 113.08, 112.39, 106.51, 68.46, 66.02, 63.51, 59.84, 59.61, 55.24, 55.19, 55.03, 54.57, 53.70, 50.21, 48.49, 39.23, 35.93, 23.16, 23.00; HRMS (ESI): calcd for $C_{52}H_{54}I_2N_2O_6^{2+}$ *m/z*: 481.1159, found: 481.1180. Yield: 69.6%.

3e N, N'-di(m-CH_3-benzyl)-Tet ammonium dibromide as a white powder. ^{1}H NMR (400 MHz, CD_3OD) δ 8.13–7.58 (m, 9H), 7.22 (s, 2H), 7.10–6.98 (m, 2H), 6.97–6.84 (m,2H), 6.71 (dd, $J = 28.6$, 14.0 Hz, 2H), 6.46 (s, 1H), 5.18 (dd, $J = 28.9$, 19.9 Hz, 2H), 4.03 (s, 2H), 4.59 (t, $J = 27.9$ Hz, 4H), 3.95–3.81 (m, 6H), 3.79–3.61 (m, 1H),3.52 (d, $J = 22.8$ Hz,3H), 3.30 (t, $J = 21.7$ Hz, 6H), 2.59 (d, $J = 22.8$ Hz, 3H); ^{13}C NMR (101 MHz, CD_3OD) δ 154.62, 154.11, 150.22, 149.84, 148.70, 146.63, 144.26, 138.67, 135.36, 134.48, 133.25, 133.02, 132.64, 132.18, 131.69, 131.23, 130.68, 130.39, 130.09, 126.10, 125.74, 125.57, 125.40, 125.31, 124.64, 123.82, 122.85, 122.68, 121.76, 121.62, 121.13, 115.91, 113.66, 113.12, 112.82, 107.13, 71.39, 70.48, 61.54, 59.83, 59.73, 55.60, 55.51, 55.30, 55.21, 54.60, 53.74, 49.51, 46.53, 41.80, 40.50, 39.49, 36.24, 23.33; HRMS (ESI): calcd for $C_{54}H_{60}N_2O_6^{2+}$ *m/z*: 416.2220, found: 416.2243. Yield: 82.3%.

3f N, N'-di(o-NO_2-benzyl)-Tet ammonium dibromide as a white powder. ^{1}H NMR (400 MHz, CD_3OD) δ 8.55–8.35 (m, 4H), 8.06 (d, $J = 7.1$ Hz, 1H), 7.90 (d, $J = 7.4$ Hz, 1H), 7.78 (t, $J = 7.9$ Hz, 1H), 7.69 (t, $J = 7.7$ Hz, 1H), 7.51 (d, $J = 8.0$ Hz, 1H), 7.17 (s, 1H), 7.02 (d, $J = 6.9$ Hz, 1H), 6.97–6.79 (m, 3H), 6.62 (d, $J = 9.4$ Hz, 2H), 6.52 (s, 1H), 6.24 (s, 1H), 5.06 (d, $J = 9.1$ Hz, 2H), 4.81–4.67 (m, 2H), 4.46 (s, 2H), 3.94 (dd, $J = 30.8$, 12.2 Hz, 2H), 3.86–3.76 (m, 6H), 3.63 (s, 2H), 3.59 (s, 3H), 3.53 (d, $J = 12.8$ Hz, 2H), 3.47 (s, 3H), 3.37 (d, $J = 24.3$ Hz, 2H), 3.30 (s, 3H), 3.21 (dd, $J = 23.3$, 12.4 Hz, 2H), 3.14–2.91 (m, 2H), 2.68 (s, 3H); ^{13}C NMR (101 MHz, CD_3OD) δ 154.76, 153.94, 150.33, 149.80, 148.70, 148.61, 146.72, 144.38, 139.44, 138.74, 138.68, 132.60, 131.69, 130.97, 130.53, 129.67, 129.15, 127.42, 126.59, 125.59, 125.49, 125.42, 124.13, 123.56, 121.81, 121.56, 121.05, 120.60, 115.54, 113.84, 113.06, 112.38, 106.65, 68.59, 66.98, 63.20, 63.14, 59.81, 55.28, 55.15, 54.74, 50.14, 39.22, 36.13, 29.38, 28.83, 23.21, 23.05; HRMS (ESI): calcd for $C_{52}H_{54}N_4O_{10}^{2+}$ *m/z*: 447.1914, found: 447.1978. Yield: 70.4%.

3 g N, N'-di(m-F-p-F-benzyl)-Tet ammonium dibromide as a white powder. ^{1}H NMR (400 MHz, CD_3OD) δ 7.66–7.53 (m, 3H), 7.44 (dd, J = 18.0, 8.5 Hz, 2H), 7.34 (q, J = 8.7 Hz, 2H), 7.17 (s, 1H), 7.07 (d, J = 7.5 Hz, 1H), 7.00–6.88 (m, 2H), 6.81 (s, 1H), 6.77–6.69 (m, 1H), 6.59 (d, J = 8.2 Hz, 1H), 6.52 (s, 1H), 6.19 (s, 1H), 5.01 (d, J = 9.6 Hz, 2H), 4.73–4.55 (m, 4H), 4.42 (d, J = 8.4 Hz, 2H), 3.94 (d, J = 13.1 Hz, 2H), 3.84 (d, J = 2.8 Hz, 6H), 3.69 (dd, J = 11.5, 4.6 Hz, 2H), 3.60 (s, 3H), 3.58–3.50 (m, 2H), 3.46 (s, 3H), 3.37 (dd, J = 18.4, 5.6 Hz, 2H), 3.30 (s, 3H), 3.24–2.90 (m, 2H), 2.70 (s, 3H); ^{13}C NMR (101 MHz, CD_3OD) δ 154.87, 153.83, 149.88, 149.77, 148.63, 146.27, 144.10, 138.62, 132.29, 131.95, 131.78, 131.14, 130.41, 129.92, 125.72, 124.51, 124.17, 123.61, 121.73, 121.38, 120.56, 118.30, 118.12, 118.06, 117.88, 115.49, 114.04, 113.01, 112.51, 106.76, 68.58, 66.44, 63.15, 59.82, 55.35, 55.27, 54.88, 53.83 53.38, 50.03, 39.19, 36.11, 23.07, 22.97; HRMS (ESI): calcd for $C_{52}H_{52}F_4N_2O_6^{2+}$ *m/z*: 438.1875. found: 438.1894, Yield: 89.4%.

3 h N, N'-di(o-CF_3-benzyl)-Tet ammonium dibromide as a white powder. ^{1}H NMR (400 MHz, CD_3OD) δ 8.06–8.02 (m, 1H), 7.98–7.81 (m, 6H), 7.78–7.68 (m, 2H), 7.20 (s, 1H), 7.15 (d, J = 8.3 Hz, 1H), 7.10–7.00 (m, 2H), 6.90 (dt, J = 18.9, 6.3 Hz, 2H), 6.79–6.67 (m, 2H), 6.46 (s, 1H), 5.24–5.13 (m, 2H), 4.69–4.46 (m, 4H), 4.19–3.91 (m, 3H), 3.88 (t, J = 7.8 Hz, 6H), 3.83–3.58 (m, 6H), 3.54 (d, J = 11.4 Hz, 3H), 3.51–3.34 (m, 4H), 3.34–3.22 (m, 6H), 3.14–2.97 (m, 2H), 2.55 (s, 3H); ^{13}C NMR (101 MHz, CD_3OD) δ 154.71, 154.14, 150.24, 149.88, 148.71, 146.55, 144.23, 138.64, 135.08, 134.36, 133.13, 132.83, 132.47, 131.90, 131.59, 131.10, 128.07, 125.97, 125.72, 125.35, 125.30, 124.55, 123.55, 122.81, 121.78, 121.74, 121.48, 121.05, 115.78, 113.61, 112.97, 112.67, 106.91, 71.13, 70.25, 61.44 ,61.33, 59.68, 55.36, 55.32, 55.10, 54.42, 53.73, 49.42, 39.42, 36.19, 29.35, 23.22, 22.84; HRMS (ESI): calcd for $C_{54}H_{54}F_6N_2O_6^{2+}$ *m/z*: 470.1938, found: 470.1944. Yield: 87.5%.

3i N, N'-di(3''-CF_3-5''-CF_3-benzyl)-Tet ammonium dibromide as a white powder. ^{1}H NMR (400 MHz, CD_3OD) δ 8.29 (dd, J = 25.0, 11.8 Hz, 6H), 7.58 (d, J = 8.3 Hz, 1H), 7.26 (s, 1H), 7.13 (d, J = 8.1 Hz, 1H), 7.05–6.95 (m, 2H), 6.90–6.84 (m, 2H), 6.71–6.60 (m, 2H), 6.22 (s, 1H), 5.08 (d, J = 9.3 Hz, 1H), 4.88 (s, 1H), 4.56 (s, 2H), 4.02 (d, J = 5.2 Hz, 2H), 3.90 (d, J = 4.2 Hz, 6H), 3.79–3.71 (m, 2H), 3.68 (s, 3H), 3.60 (d, J = 9.3 Hz, 2H), 3.55 (s, 3H), 3.41–3.35 (m, 2H), 3.31 (d, J = 5.7 Hz, 4H), 3.09 (d, J = 14.7 Hz, 2H), 2.79 (s, 3H); ^{13}C NMR (101 MHz, CD_3OD) δ 155.10, 154.08, 150.39, 149.87, 148.87, 146.44, 144.54, 138.50, 138.28, 133.06, 132.85, 132.63, 132.52, 132.37, 132.29, 132.18, 131.95, 131.84, 131.61, 131.30, 130.95, 130.87, 130.31, 125.74, 124.57, 124.35, 124.27 , 123.94, 123.86, 122.04, 121.64, 121.56, 121.35, 121.03, 120.87, 115.11, 114.22, 112.89, 112.43, 106.72, 68.81, 67.49, 62.88, 62.74, 59.60, 55.27, 55.16, 53.75, 50.06, 39.21, 35.98, 23.19, 22.99; HRMS (ESI): calcd for $C_{56}H_{52}F_{12}N_2O_6^{2+}$ *m/z*: 538.1811, found: 538.1822, Yield: 91.5%.

3j N, N'-di(2''-F-5''-CF_3 -benzyl)-Tet ammonium dibromide as a white powder. ^{1}H NMR (400 MHz, CD_3OD) δ 8.15 (d, J = 5.3 Hz, 1H), 8.04 (d, J = 5.3 Hz, 3H), 7.65 (ddd, J = 21.7, 17.3, 8.8 Hz, 3H), 7.21 (d, J = 8.9 Hz, 2H), 7.06–6.97 (m, 2H), 6.90–6.83 (m, 2H), 6.67 (d, J = 11.8 Hz, 2H), 6.26 (s, 1H), 5.10 (dd, J = 28.3, 7.3 Hz, 2H), 4.73–4.48 (m, 4H), 4.14–3.97 (m, 2H), 3.89 (d, J = 5.0 Hz, 6H), 3.86–3.75 (m, 2H), 3.64 (s, 6H), 3.57 (d, J = 13.8 Hz, 4H), 3.49–3.33 (m, 2H), 3.29 (d, J = 8.8 Hz, 3H), 3.13 (dd, J = 77.3, 13.2 Hz, 2H), 2.85 (s, 3H); ^{13}C NMR (101 MHz, CD_3OD) δ 165.68, 165.48, 163.14, 162.92, 154.82, 154.07, 150.31, 149.80, 148.75, 146.76, 144.36, 138.57, 132.61, 131.90, 131.65, 131.65, 130.98, 127.51, 125.47, 124.83, 124.71, 124.07, 123.94, 122.13, 122.08, 122.01, 121.21, 117.98, 117.74, 116.6, 116.52, 116.42, 116.26, 115.46, 114.23, 112.54, 112.47, 106.69, 69.67, 67.75, 59.79, 57.82, 55.41, 55.32, 54.87, 54.05, 49.44, 39.36, 36.33, 23.22, 23.16; HRMS (ESI): calcd for $C_{54}H_{52}F_8N_2O_6^{2+}$ *m/z*: 488.1843, found: 488.1832. Yield: 80.4%.

4.1.3. Demethylation from tetrandrine to obtain fangchinoline

Tetrandrine (100 mg, 0.16 mM) was dissolved in a mixed solution of 1.5 mL of hydrobromic acid and 2.5 glacial acetic acid and stirred at 90 °C for 8 h. After the solution was cooled to room temperature, it was neutralized with a saturated Na_2CO_3 solution. The extract was extracted with CH_2Cl_2, and the obtained CH_2Cl_2 layer was concentrated by rotary evaporation. The residue was purified by column chromatography, and fangchinoline was obtained by using CH_2Cl_2/CH_3OH as the eluent.

d-Tet as a white powder. ^{1}H NMR (400 MHz, $CDCl_3$) δ 7.21 (d, J = 8.0 Hz, 1H), 7.03 (dd, J = 8.1, 1.5 Hz, 1H), 6.70 (dd, J = 12.8, 4.7 Hz, 3H), 6.49 (s, 1H), 6.39 (s, 1H), 6.18 (d, J = 5.0 Hz, 2H), 5.96 (s, 1H), 3.80 (s, 3H), 3.77–3.72 (m, 1H), 3.68 (d, J = 9.7 Hz, 1H), 3.62 (s, 3H), 3.44–3.27 (m, 2H), 3.22 (s, 3H), 3.17–3.02 (m, 2H), 2.79 (td, J = 17.3, 6.5 Hz, 4H), 2.69–2.56 (m, 4H), 2.46 (s, 3H), 2.22 (s, 3H); ^{13}C NMR (101 MHz, $CDCl_3$) δ 173.38, 153.70, 149.24, 148.86, 146.92, 146.49, 143.99, 142.62, 135.10, 135.05, 132.59, 130.18, 129.89, 128.11, 127.59, 123.37, 122.87, 122.77, 121.80, 120.84, 116.16, 112.76, 111.51, 104.97, 63.54, 61.48, 56.07, 56.03, 55.94, 53.59, 44.99, 44.14, 42.24, 38.03, 25.04, 22.39, 21.81; HRMS (ESI): calcd for $C_{54}H_{52}F_8N_2O_6^{2+}$ *m/z*: 608.2886, found: 609.2910 $[M + H]^+$. Yield: 51.5%.

4.1.4. Synthesis of substituted phenyl fangchinoline derivatives

A mixture of fangchinoline (100 mg, 0.16 mM) and NaH (20 mg, 0.83 mM) was dissolved in 2 mL of DMF at 0 °C under argon protection. R_1CH_2Br (0.18 mM) was added dropwise slowly. TLC analysis was performed until completion of the reaction, and the solution was concentrated by rotary evaporation. The residue was purified by column chromatography on silica, eluting to afford **4a-4b** using CH_2Cl_2/CH_3OH as the eluent.

4a 7-*O*-(m-SCF_3)-*d*-Tet as a white powder. ^{1}H NMR (400 MHz, $CDCl_3$) δ 7.54 (d, J = 6.6 Hz, 2H), 7.34 (d, J = 6.8 Hz, 1H), 7.16 (d, J = 6.3 Hz, 1H), 7.03 (d, J = 6.6 Hz, 2H), 6.94–6.75 (m, 3H), 6.55 (s, 2H), 6.36 (s, 2H), 5.93 (s, 1H), 4.67 (d, J = 10.9 Hz, 1H), 4.30 (d, J = 11.0 Hz, 1H), 3.95 (s, 3H), 3.74 (s, 3H), 3.55 (d, J = 12.1 Hz, 2H), 3.41 (s, 3H), 3.24 (d, J = 7.8 Hz, 2H), 3.11–2.59 (m, 8H), 2.52 (s, 3H), 2.36 (s, 3H); ^{13}C NMR (101 MHz, $CDCl_3$) δ 153.65, 151.25, 149.38, 148.73, 148.44, 147.02, 143.84, 140.68, 136.42, 136.07, 135.33, 134.79, 132.66, 131.17, 130.14, 128.67, 128.11, 127.60, 123.24, 122.94, 122.73 , 121.94 , 120.13, 116.09, 112.91, 111.47, 105.93, 73.18, 63.99, 61.44, 56.12, 55.95, 55.77, 45.68, 44.05, 42.63, 42.34, 41.99, 38.82, 25.61, 22.03; HRMS (ESI): calcd for $C_{45}H_{45}F_3N_2O_6S$ *m/z*: 798.2950, found: 799.2923 $[M + H]^+$. Yield: 87.1%.

4b 7-*O*-(o-Cl-p-F)-*d*-Tet as a white powder. ^{1}H NMR (400 MHz, $CDCl_3$) δ 7.32 (d, J = 8.1 Hz, 1H), 7.15 (dd, J = 8.1, 2.2 Hz, 1H), 7.01 (d, J = 8.4 Hz, 1H), 6.91 (dd, J = 12.8, 4.5 Hz, 4H), 6.85–6.79 (m, 1H), 6.54 (d, J = 11.1 Hz, 2H), 6.39–6.28 (m, 2H), 5.84 (s, 1H), 4.64 (d, J = 12.6 Hz, 1H), 4.50 (d, J = 12.6 Hz, 1H), 3.94 (s, 3H), 3.73 (s, 3H), 3.69–3.45 (m, 4H), 3.40 (d, J = 6.0 Hz, 3H), 3.30–3.13 (m, 2H), 2.94 (dd, J = 10.2, 4.9 Hz, 2H), 2.84–2.65 (m, 6H), 2.44 (d, J = 7.5 Hz, 3H), 2.36 (s, 3H); ^{13}C NMR (101 MHz, $CDCl_3$) δ 162.75, 153.67, 151.35, 149.38, 148.74, 148.27, 147.04, 143.80, 136.37, 135.28, 134.82, 132.65, 132.05, 130.12, 129.82, 129.74, 128.75, 128.50, 123.28, 122.78, 121.91, 120.26, 116.17,115.92, 115.67, 113.89, 113.68, 112.83, 111.50, 105.95, 70.13, 63.79, 61.47, 56.11, 55.92, 55.75, 45.56, 44.08, 42.41, 42.34, 41.99, 38.66, 25.59, 22.02; HRMS (ESI): calcd for $C_{44}H_{44}ClFN_2O_6$ *m/z*: 750.2872, found: 751.2957 $[M + H]^+$. Yield: 91.5%.

4.1.5. Synthesis of sulfonyl fangchinoline derivatives

A mixture of fangchinoline (100 mg, 0.16 mM) and pyridine (55 mg, 0.64 mM) was dissolved in 2 mL of CH_2Cl_2 at 0 °C under argon protection, followed by the slow addition of R_3SO_2Cl (0.18 mM). TLC analysis was performed until completion of the reaction, and the solution was concentrated by rotary evaporation. The residue was purified by column chromatography, and **4c-4j** was obtained by using CH_2Cl_2/CH_3OH as the eluent.

4c 7-*O*-(CH_3-sulfonyl)-*d*-Tet as a light-yellow powder. ^{1}H NMR (400 MHz, $CDCl_3$) δ 7.40 (dd, J = 8.2, 1.9 Hz, 1H), 7.15 (dd, J = 8.2, 2.5 Hz,

1H), 6.85 (d, $J = 7.7$ Hz, 2H), 6.81 (dd, $J = 8.3$, 2.5 Hz, 1H), 6.56 (s, 1H), 6.46 (s, 1H), 6.40 (s,1H), 6.33 (dd, $J = 8.3$, 2.0 Hz, 1H), 6.04 (s, 1H), 3.92 (s, 3H), 3.78 (s, 3H), 3.70 (dd, $J = 22.5$, 12.4 Hz, 2H), 3.52 (dd, $J = 16.1$, 12.9 Hz,2H), 3.43–3.36 (m, 3H), 2.99 (tdd, $J = 18.0$, 13.2, 6.7 Hz, 6H), 2.87 (d, $J = 8.4$ Hz, 3H), 2.81 (dd, $J = 13.8$, 6.1 Hz, 2H), 2.69 (d, $J = 9.0$ Hz, 3H), 2.60–2.45 (m, 2H), 2.30 (s, 3H); ^{13}C NMR (101 MHz, $CDCl_3$) δ 154.05, 150.13, 149.26, 148.93, 148.67, 147.04, 142.47, 134.36, 133.63, 132.65, 130.52, 127.64, 127.09, 125.34 , 123.40, 122.98, 122.30, 122.05, 121.91, 115.88, 112.33, 111.54, 106.14, 64.38, 61.37, 56.10, 56.01, 55.80, 45.84, 44.89, 43.77, 42.29, 41.83, 41.37, 39.53, 39.12, 23.39, 22.12; HRMS (ESI): calcd for $C_{38}H_{42}N_2O_8S$ *m/z*: 686.2662, found: 687.2711 $[M + H]^+$. Yield: 95.4%.

4d 7-*O*-(CH_2CH_3-sulfonyl)-*d*-Tet as a light-yellow powder. ^{1}H NMR (400 MHz, $CDCl_3$) δ 7.36 (dd, $J = 8.2$, 1.9 Hz, 1H), 7.14 (dd, $J = 8.2$, 2.4 Hz, 1H), 6.82 (dt, $J = 8.3$, 5.3 Hz, 3H), 6.51 (d, $J = 16.7$ Hz, 2H), 6.42–6.30 (m, 2H), 6.04 (s, 1H), 3.92 (s, 3H), 3.88–3.81 (m, 1H), 3.81–3.73 (m, 3H), 3.69 (s, 1H), 3.62–3.41 (m, 3H), 3.37 (d, $J = 11.3$ Hz, 3H), 3.31–3.11 (m, 2H), 3.08–2.64 (m, 10*H*), 2.59 (s, 3H), 2.47 (ddd, $J = 36.1$, 25.3, 16.1 Hz, 2H), 2.35–2.23 (m, 3H), 1.26 (t, $J = 7.4$ Hz, 3H); ^{13}C NMR (101 MHz, $CDCl_3$) δ 153.58, 150.32, 149.36, 148.89, 148.10, 146.92, 142.25, 135.08, 134.46, 132.51, 132.40, 130.42, 128.47,128.30, 127.70, 123.67, 122.78, 122.12, 121.94, 121.41, 115.79, 112.60, 111.39, 106.14, 63.94, 61.37, 56.08, 56.06, 55.86, 46.42, 46.02, 45.14, 43.71, 42.46, 42.30, 41.47, 38.94, 24.77, 22.14; HRMS (ESI): calcd for $C_{39}H_{44}N_2O_8S$ *m/z*: 700.2818, found: 701.2892 $[M + H]^+$. Yield: 90.6%.

4e 7-*O*-($CH_3CH_2CH_2$-sulfonyl)-*d*-Tet as a light-yellow powder. ^{1}H NMR (400 MHz, $CDCl_3$) δ 7.29 (dd, $J = 8.2$, 1.9 Hz, 1H), 7.06 (dd, $J = 8.1$, 2.4 Hz, 1H), 6.74 (dt, $J = 8.3$, 5.4 Hz, 3H), 6.43 (d, $J = 14.0$ Hz, 2H), 6.36–6.19 (m, 2H), 5.96 (s, 1H), 3.84 (s, 3H), 3.76 (dd, $J = 11.1$, 5.3 Hz, 0H), 3.73–3.65 (m, 3H), 3.62 (d, $J = 9.7$ Hz, 0H), 3.40 (ddd, $J = 11.9$, 9.6, 5.7 Hz, 1H), 3.26 (d, $J = 14.9$ Hz, 3H), 2.93–2.74 (m, 2H), 2.70–2.59 (m, 1H), 2.57–2.45 (m, 1H), 2.23 (d, $J = 16.7$ Hz, 1H), 1.76–1.57 (m, 1H), 0.89 (t, $J = 7.5$ Hz, 1H); ^{13}C NMR (101 MHz, $CDCl_3$) δ 153.60, 150.38, 149.37, 148.97, 148.10, 146.92, 142.25, 135.16, 134.52, 132.46, 130.42, 128.42, 127.63, 123.67, 122.78, 122.15, 121.95, 121.55, 115.84, 112.60, 111.38, 106.14, 64.04, 61.39, 56.09, 56.08, 55.87, 53.46, 45.19, 43.74, 42.41, 41.52, 39.23, 29.72, 24.73, 22.11, 17.16, 12.91; HRMS (ESI): calcd for $C_{40}H_{46}N_2O_8S$ *m/z*: 714.2975, found: 715.3008 $[M + H]^+$. Yield: 91.5%.

4f 7-*O*-(benzene-sulfonyl)-*d*-Tet as a light-yellow powder. ^{1}H NMR (400 MHz, $CDCl_3$) δ 7.66 (dd, $J = 15.5$, 7.8 Hz, 4H), 7.47 (t, $J = 7.4$ Hz,2H), 7.33 (d, $J = 8.1$ Hz, 1H), 7.16 (dd, $J = 8.1$, 1.4 Hz, 1H), 6.88 (s, 2H), 6.78–6.72 (m, 1H), 6.51–6.44 (m, 2H), 6.32–6.20 (m, 2H), 3.93 (s, 3H), 3.69 (dd, $J = 15.9$, 7.6 Hz, 2H), 3.52 (dd, $J = 19.7$, 9.0 Hz, 2H), 3.44 (s, 3H), 3.27 (d, $J = 12.0$ Hz, 3H), 3.26–3.12 (m, 2H), 2.97–2.87 (m, 4H), 2.74 (dd, $J = 16.4$, 7.2 Hz, 2H), 2.63 (d, $J = 6.5$ Hz, 4H), 2.47 (dd, $J = 17.6$, 12.5 Hz, 2H), 2.29 (s, 3H); ^{13}C NMR (101 MHz, $CDCl_3$) δ 153.75, 150.99, 149.31, 148.87, 147.75, 147.12, 142.39 ,137.39, 135.25, 135.03, 134.60, 133.56, 132.52, 130.25, 128.58, 128.36, 128.19, 128.11, 123.77, 122.85, 121.69, 121.03, 116.08, 112.70, 111.52, 106.00, 77.45, 77.19, 76.87, 63.87, 61.37, 56.13, 55.78, 55.69, 45.08, 43.85, 42.39, 42.03, 39.77, 24.30, 22.04; HRMS (ESI): calcd for $C_{43}H_{44}N_2O_8S$ *m/z*: 748.2852 found: 749.2864 $[M + H]^+$. Yield: 87.8%.

4 g 7-*O*-(2-Br-benzene-sulfonyl)-*d*-Tet as a light-yellow powder. ^{1}H NMR (400 MHz, $CDCl_3$) δ 7.79 (t, $J = 1.6$ Hz, 1H), 7.70 (d, $J = 8.0$ Hz, 1H), 7.51 (d, $J = 8.0$ Hz, 1H), 7.38–7.16 (m, 3H), 7.10 (dd, $J = 8.1$, 2.5 Hz, 1H), 6.83–6.77 (m, 2H), 6.66 (dd, $J = 8.3$, 2.5 Hz, 1H), 6.38 (d, $J = 7.2$ Hz, 2H), 6.25 (s, 1H), 6.17 (dd, $J = 8.3$, 2.0 Hz, 1H), 3.83 (d, $J = 9.4$ Hz, 3H), 3.65 (dd, $J = 11.1$, 5.4 Hz, 1H), 3.57 (d, $J = 9.9$ Hz, 1H), 3.45 (s, 3H), 3.43–3.31 (m, 2H), 3.20 (s, 3H), 2.96–2.59 (m, 8H), 2.55 (s, 3H), 2.43 (dd, $J = 30.0$, 9.4 Hz, 2H), 2.20 (s, 3H); ^{13}C NMR (101 MHz, $CDCl_3$) δ 153.77, 150.96, 149.26, 148.70, 147.61, 147.12, 142.29, 139.25, 136.62, 135.06, 134.51, 132.69, 131.39, 130.17, 128.53, 128.32, 127.98, 127.22, 123.98, 122.85, 122.46, 121.77, 120.61, 116.26, 112.81, 111.47, 106.22, 63.74, 61.38, 56.11, 55.80, 46.14, 45.02, 43.80, 42.37, 39.64, 24.33, 22.00; HRMS (ESI): calcd for $C_{43}H_{43}BrN_2O_8S$ *m/z*: 826.1923, found: 827.1965 $[M + H]^+$. Yield: 83.5%.

4 h 7-*O*-(2-F-benzene-sulfonyl)-*d*-Tet as a light-yellow powder. ^{1}H NMR (400 MHz, $CDCl_3$) δ 7.63 (d, $J = 6.8$ Hz, 2H), 7.40–7.07 (m, 5H), 6.86 (s, 2H), 6.75 (d, $J = 7.8$ Hz, 1H), 6.49 (s, 2H), 6.26 (d, $J = 13.2$ Hz, 2H), 3.91 (s, 3H), 3.67 (t, $J = 10.0$ Hz, 2H), 3.48 (d, $J = 10.5$ Hz, 2H), 3.38 (s, 3H), 3.30 (s, 3H), 2.79 (ddd, $J = 33.4$, 22.7, 13.2 Hz, 8H), 2.60 (s, 3H), 2.57–2.34 (m, 2H), 2.28 (s, 3H); ^{13}C NMR (101 MHz, $CDCl_3$) δ 166.95, 153.77, 150.89, 149.39, 148.74, 147.81, 147.14, 142.32, 134.98, 134.45, 133.49, 132.61, 131.43, 130.22, 128.31, 128.11, 127.74, 123.84, 122.82, 121.85, 120.72, 116.02, 115.96, 115.79, 112.73, 111.52, 106.04, 63.98, 61.35, 56.13, 55.77, 45.05, 43.85, 42.39, 42.09, 39.20, 24.49, 22.08; HRMS (ESI): calcd for $C_{43}H_{43}FN_2O_8S$ *m/z*: 766.2724, found: 767.2717 $[M + H]^+$. Yield: 89.3%.

4i 7-*O*-(4-Cl-benzene-sulfonyl)-*d*-Tet as a white powder. ^{1}H NMR (400 MHz, $CDCl_3$) δ 7.52 (d, $J = 8.6$ Hz, 2H), 7.47–7.27 (m, 4H), 7.11 (dd, $J = 8.1$, 2.4 Hz, 1H), 6.79 (s, 2H), 6.68 (dd, $J = 8.2$, 2.4 Hz, 1H), 6.37 (d, $J = 12.4$ Hz, 2H), 6.26–6.18 (m, 2H), 3.86 (s, 3H), 3.62–3.54 (m, 2H), 3.45 (s, 3H), 3.33 (ddd, $J = 23.1$, 12.3, 8.9 Hz, 2H), 3.21 (s, 3H), 2.92–2.62 (m, 8H), 2.57 (s, 3H), 2.49–2.37 (m, 2H), 2.20 (s, 3H); ^{13}C NMR (101 MHz, $CDCl_3$) δ 153.64, 150.93, 149.42, 148.61, 147.68, 147.10, 142.23, 140.15, 135.93, 135.10, 134.40, 132.60, 130.30, 130.05, 129.34, 128.92, 128.50, 128.37, 128.21, 128.02, 123.80, 122.77, 121.87, 120.41, 115.80, 112.79, 111.49, 106.13, 63.96, 61.37, 56.07, 55.79, 53.54, 45.08, 43.84, 42.54, 42.34, 42.04, 39.15, 24.58, 22.12; HRMS (ESI): calcd for $C_{43}H_{43}ClN_2O_8S$ *m/z*: 782.2829, found: 783.2862 $[M + H]^+$. Yield: 81.2%.

4j 7-*O*-(2-Naphthalene-sulfonyl)-*d*-Tet as a light-yellow powder. ^{1}H NMR (400 MHz, $CDCl_3$) δ 8.20 (s, 1H), 8.02–7.75 (m, 4H), 7.69 (t, $J = 7.5$ Hz, 1H), 7.56 (dd, $J = 15.4$, 8.1 Hz, 2H), 6.85–6.73 (m, 3H), 6.61 (d, $J = 7.4$ Hz, 1H), 6.54 (dd, $J = 8.2$, 2.1 Hz, 1H), 6.30 (d, $J = 23.5$ Hz, 2H), 6.21 (s, 1H), 6.03 (d, $J = 8.2$ Hz, 1H), 4.40 (s, 1H), 3.84 (s, 3H), 3.53 (d, $J = 10.0$ Hz, 1H), 3.45 (d, $J = 10.1$ Hz, 3H), 3.33 (ddd, $J = 21.6$, 20.7, 10.6 Hz, 2H), 3.19 (d, $J = 14.4$ Hz, 3H), 2.94–2.68 (m, 6H), 2.53 (s, 3H), 2.51–2.31 (m, 4H), 2.20 (d, $J = 12.1$ Hz, 3H); ^{13}C NMR (101 MHz, $CDCl_3$) δ 153.47, 151.48, 149.29, 148.57, 147.57, 147.12, 142.42, 135.28, 134.63, 134.59, 134.47, 132.42, 131.87, 129.97, 129.52, 128.73, 128.08, 127.79, 127.59, 123.85, 122.83, 121.50, 120.04, 115.89, 112.84, 111.47, 106.42, 63.42, 61.42, 56.12, 56.59, 55.77, 44.96, 43.91, 42.41, 42.32, 42.23, 39.05, 24.34, 22.05; HRMS (ESI): calcd for $C_{47}H_{46}N_2O_8S$ *m/z*: 798.2975, found: 799.3029 $[M + H]^+$. Yield: 82.4%.

4.2. Cell culture

A549, HeLa, MCF-7, HepG-2, and H460 cells were purchased from the Cell Bank of Type Culture Collection of the Chinese Academy of Sciences (Shanghai, China). H520 cells and BEAS-2B cells were purchased from the American Type Culture Collection (ATCC; Manassas, VA, USA). The cells were maintained in medium (HyClone) containing 10% fetal bovine serum (Gibco) and 100 U/mL penicillin–streptomycin (HyClone). All cells were cultured under humid conditions at 37 ℃, 95% air and 5% CO_2.

4.3. CCK-8 assays

A549 cells in the logarithmic growth phase were seeded on a 96-well plate for 12 h at a density of 5000 cells/well. The cells were treated with different concentrations of 20, 10, 5, 2.5, 1.25, 0.625 and 0.165 μM for 24, 48, and 72 h. At the end of the incubation, 10 μL of CCK-8 (10 mg/mL) and 90 μL of the medium were added to each pore, and the plate was placed at 37 °C for 2 h. The absorbance was measured at 450 nm using a microplate reader (BIO-RAD, USA).

4.4. Colony formation assays

A total of 1000 cells in the logarithmic growth phase were inoculated in 6-cm Petri dishes. One week later, the cells were treated with different concentrations of compound **4 g** medium. The cells were cultured for two weeks. The plates were washed with PBS, fixed with 4% paraformaldehyde and stained with Giemsa (0.04%).

4.5. Flow cytometry

Flow cytometry was used to analyze the cell cycle and induce apoptosis in A549 cells. For cycle detection, A549 cells were treated with **4g** at 0, 1, 2, and 3 μM for 48 h, and the cells were harvested and plated in 70% ethanol. The cells were fixed overnight at 4 °C and then treated with 500 μL of RNase/propidium iodide (PI) solution for 40 min in the dark, and the cell cycle was measured by flow cytometry. For apoptosis detection, A549 cells were treated with **4g** at concentrations of 0, 1, 2, and 3 μM for 48 h, and cells were collected for staining with FITC Annexin V and PI. The stained cells were detected by FACSCalibur (BD Biosciences).

4.6. Cell migration and invasion assay

Cancer cell migration was assessed using a cell wound healing assay. For wound healing assays, A549 cells were incubated in a 6-well plate at 37 °C for 24 h to form a confluent cell monolayer, and the wound was scratched with a sterile pipette tip and photographed with an inverted microscope (Olympus Corp, Tokyo, Japan). A549 cells were treated with 0, 1, 2, or 3 μM **4g** for 48 h, and photographs were taken again. Cell invasion was assessed by Transwell analysis. Briefly, a 24-well Transwell chamber was precoated with 70 μL of diluted Matrigel (diluted 1:2 with serum-free medium) in the upper chamber. A549 cells (1×10^5 well) were seeded in the upper chamber and treated with 0, 1, 2, or 3 μM **4g**. The lower chamber was filled with RPMI-1640 supplemented with 10% FBS and 1% penicillin/streptomycin at 37 °C and 5% CO_2. After 24 h of incubation, cells that passed through the chamber were fixed with 4% paraformaldehyde for 30 min at room temperature and stained with crystal violet for 20 min. Finally, photographs were taken under an inverted microscope (Olympus Corporation, Tokyo, Japan).

4.7. Hoechst 33,258 staining

Cells (5×10^4 cells/well) were inoculated on a 12-well culture plate and incubated with **4g** of various concentrations for 48 h. Then, the cells were washed with PBS, fixed for 15 min (4% paraformaldehyde), stained with Hoechst 33,258 for 5 min (1 μg/mL), and then washed twice with PBS. Finally, the apoptotic characteristics of the cancer cells were studied using confocal microscopy (SP8, Leica, GER).

4.8. Mitochondrial membrane potential (ΔΨm) measurements

The changes in MMP were quantified by JC-1 assay. Healthy polarized cell mitochondria form JC-1 aggregates (green fluorescence), while dead cells form JC-1 monomers (red fluorescence). Cells (5×10^4 cells/pore) were inoculated on a 12-well plate and incubated with various concentrations of **4g** for 48 h. Then, the cells were washed with PBS and terminated according to the manufacturer's instructions. The results were detected using fluorescence microscopy (SP8, Leica, GER).

4.9. Western blot analysis

A549 cells were treated with or without **4g** (1×10^6 cells/well on 6-well plates). The total protein concentration of each sample was estimated using the BCA protein kit. A total of 80 μg of protein was electrophoretically separated by 12% or 10% SDS-PAGE and transferred to a nitrocellulose membrane. The membrane was then blocked with 5% skimmed milk for 1 h and incubated overnight with the appropriate primary antibodies overnight at 4 °C with appropriate dilutions. After incubation, the membrane was washed with TBST and incubated with two antibodies. Finally, the imprinting was developed using an enhanced chemiluminescence detection kit, and the relative protein expression level was quantified using ImageJ software.

4.10. Statistical analysis

All experimental data are reported as the mean value of the specified number of independent experiments plus the standard deviation (SD). The data are expressed as an average value of ± SD. $P < 0.05$ (*) was considered to be statistically significant. Additionally, $P < 0.01$ (**) and $P < 0.001$ (***) are statistically significant.

Declaration of Competing Interest

The authors declare that they have no conflicts of interest.

Acknowledgement

This study was supported by the National Natural Science Foundation of China (No. 82003632); the Natural Science Foundation of Shandong, China (No. ZR2020MH401); the Provincial Major Scientific and Technological Innovation Project of Shandong, China (NO. 2019JZZY020612); the Province Agricultural Major Application Technology Innovation Project of Shandong, China (NO. SD2019ZZ016); the Provincial Key Research and Development Program of Shandong, China (NO. 2019LYXZ025, 2019GSF109087); the Taishan Scholars's Program of Shandong for Jinyue Sun.

Appendix A. Supplementary data

Supplementary data to this article can be found online at https://doi.org/10.1016/j.bioorg.2021.104694.

References

[1] R.L. Siegel, K.D. Miller, A. Jemal, Cancer statistics, 2020, CA. Cancer J. Clin. 70 (2020) 7–30.
[2] F. Bray, J. Ferlay, I. Soerjomataram, R.L. Siegel, L.A. Torre, A. Jemal, Global cancer statistics,2018: Globocan estimates of incidence and mortality worldwide for 36 cancers in 185 countries, CA. Cancer J. Clin. 68 (2018) (2018) 394–424.
[3] World health organization. World cancer report 2014.
[4] M. Asher, Cancer market hits $100 billion, Nature 14 (2015) 373.
[5] R. Kumar, K. Chaudhary, S. Gupta, H. Singh, S. Kumar, A. Gautam, P. Kapoor, Cancer DR: Cancer Drug Resistance Database, Sci. Rep. 3 (2013) 1445–1451.
[6] F. Gao, X. Zhang, T.F. Wang, J.Q. Xiao, Quinolone hybrids and their anti-cancer activities: an overview, Eur. J. Med. Chem. 165 (2019) 59–79.
[7] H.J. Zhao, X. Liu, Novel myricetin derivatives: design, synthesis and anticancer activity, Eur. J. Med. Chem. 5 (2015) 155–163.
[8] H.J. Zeng, R. Yang, L.F. Lei, Y.P. Wang, National Pharmacopoeia Committee, Chinese Med. 6 (2015) 359.
[9] L.N. Gao, Q.S. Feng, X.F. Zhang, Q.S. Wang, Y.L. Cui, Tetrandrine suppresses articular inflammatory response by inhibiting pro-inflammatory factors via NF-κB inactivation, J. O. rthop. Res. 34 (2016) 1557–1568.
[10] T. Liu, Q.X. Zeng, X.Q. Zhao, W. Wei, Y.H. Li, H.B. Deng, D.Q. Song, Synthesis and biological evaluation of fangchinoline derivatives as anti-inflammatory agents through inactivation of inflammasome, Molecules 24 (2019) 1154–1170.
[11] P. Joshi, R.A. Vishwakarma, S.B. Bharate, Natural alkaloids as P-gp inhibitors for multidrug resistance reversal in cancer, Eur. J. Med. Chem. 138 (2017) 273–292.
[12] D.C. Li, Z.H. Liu, Y.F. Liu, Q.K. Zhang, C. Liu, S.H. Zhao, B. Jiao, Design, synthesis and biological activities of tetrandrine and fangchinoline derivatives as antitumer agents, Bioorg. Med. Chem. Lett. 27 (2017) 533–536.
[13] J.J. Lan, N. Wang, L. Huang, Y.Z. Liu, X.P. Ma, H.Y. Lou, C. Chen, Y.B. Feng, W. D. Pan, Design and synthesis of novel tetrandrine derivatives as potential anti-tumor agents against human hepatocellular carcinoma, Eur. J. Med. Chem. 127 (2017) 554–566.
[14] J. Yang, S.C. Hu, C.L. Wang, J.R. Song, W.D. Pan, Fangchinoline derivatives induce cell cycle arrest and apoptosis in human leukemia cell lines via suppression of the PI3K/AKT and MAPK signaling pathway, Eur. J. Med. Chem. 186 (2020), 111898.
[15] Y.C. Zhang, X.Z. Gao, C. Liu, M.X. Wang, R.R. Zhang, J.Y. Sun, Y.F. Liu, Design, synthesis and in vitro evaluation of fangchinoline derivatives as potential anticancer agents, Bioorg. Chem. 94 (2020), 103431.

[16] H.L. Wang, X.H. Zhang, Y. Hong, X. Jin, D.R. Zhang, Tetrandrine prevents monocrotaline-induced pulmonary hypertension in rats, Drug. Develop. Res. 39 (2015) 158–160.
[17] L.Z. Yu, C.R. Shi, Effect of tetrandrine on myocardial hypertrophy in renal hypertension rats and its mechanism of action, Int. J. Tradit. Chin. Med. 35 (2013) 785–788.
[18] F.X. Bao, L.X. Tao, H.Y. Zhang, Neuroprotective effect of natural alkaloid fangchinoline against oxidative glutamate toxicity: Involvement of Keap1-Nrf2 axis regulation, Cell Mol. Neurobiol 39 (2019) 1177–1186.
[19] I. Gulicin, R. Elias, A. Gepdiremen, A. Chea, F. Topal, Antioxidant activity of bisbenzylisoquinoline alkaloids from Stephania rotunda: cepharanthine and fangchinoline, J. Enzym. Inhib. Med. Ch. 25 (2010) 44–53.
[20] Z. Wu, Effect of tetrandrine on intracelluar Ca^{2+} overload of cultured rat cardiomyocytes during hypoxia and reoxygenation, Clin. Cardiol 16 (2000) 83–84.
[21] Y. Zhang, Q. Wang, Sunitinib reverse multidrug resistance ingastriccancer cells by modulating stat3 and inhibiting P-gp function, Cell Biochem. Biophys. 67 (2013) 575–581.
[22] Y.F. Sun, M. Wink, Tetrandrine and fangchinoline, bisbenzyli- soquinoline alkaloids from Stephania tetrandra can reverse multidrug resistance by inhibiting P-glycoprotein activity in multidrug resistant human cancer cells, Phytomedicine 21 (2014) 1110–1119.
[23] P. He, F.P. Wang, Partial synthesisand biological evaluation of bisbenzylisoquinoline alkaloids derivatives: potential modulators of multidrug resistance in cancer, J. Asian. Nat. Prod. Res. 14 (2012) 564–576.
[24] H.L. Shen, W.L. Xu, Q.Y. Chen, Z.Y. Wu, H.R. Tang, F.C. Wang, Tetrandrine prevents acquired drug resistance of K562 cells through inhibition of mdr1 gene transcription, J. Cancer Res. Clin. 136 (2010) 659–665.
[25] P.L. Kuo, C.C. Lin, Tetrandrine induced cell cycle arrest and apoptosis in $HepG_2$ cells, Sci. China Life 73 (2003) 243–252.
[26] R.H. Zhu, T.Y. Liu, Z.J. Tan, X.S. Wu, Y.B. Liu, Tetrandrine induces apoptosis in gallbladder carcinoma *in vitro*, Int. J. Clin. Pharmacol Ther. 52 (2014) 900–905.
[27] R. Qin, H.L. Shen, Y. Cao, Y. Fang, H. Li, Q.Y. Chen, W.L. Xu, Tetrandrine induces mitochondria mediated apoptosis in human gastric cancer BGC-823 cells, Plos. 8 (2013) 476–486.
[28] K. Gong, C. Chen, Y. Zhan, Y. Chen, Z. Huang, W. Li, Autophagy-related gene7 (ATG7) and reactive oxygen species extracellular signal-regulated kinase regulate tetrandrine-induced autophagy in human hepatocellular carcinoma, J. Biol. Chem. 287 (2012) 35576–35588.
[29] H. Sun, X.D. Liu, Q. Liu, F.P. Wang, X.Q. Bao, D. Zhang, Reversal of P-glycoprotein-mediated multidrugresistance by the novel tetrandrine derivative W6, J. Asian. Nat. Prod. Res. 17 (2015) 638–648.
[30] E. Wolmarans, T.V. Mqoco, A. Stander, S.D. Nkandeu, K. Sippel, R. Mckenna, A. Joubert, Novel estradiol analogue induces apoptosis and autophagy in esophageal carcinoma cells, Cell Mol. Biol. 19 (2014) 98–115.
[31] A. Yang, I. Hacheney, Y.W. Wu, Semisynthesis of autophagy protein LC3 conjugates, Bioorg. Med. Chem. Lett 25 (2017) 4971–4976.
[32] Z.B. Xing, L. Yao, G.Q. Zhang, Fangchinoline inhibits breasr adenocarcinoma proliferation by inducting apoptosis, Chem. Pharm. Bull. 59 (2011) 1476–1480.
[33] A. Roda, C. Cerrè, A.C. Manetta, G. Cainelli, A. Umani-ronchi, M. Panunzio, Synthesis physicochemical biological and pharmacological properties of new bile acids amidated with cyclic amino acids, J. Med. Chem. 27 (1996) 2270–2276.
[34] T.D. Penning, J.J. Talley, S.R. Bertenshaw, Synthesis and biological evaluation of the 1,5-diarylpyrazole class of cyclooxygenase-2 inhibitors: identification of 4-[5-(4-methylphenyl)-3-(trifluoromethyl) -1H-pyrazol-1-yl]benzenesulfonamide (SC-58635, celecoxib), Cheminform 28 (2010) 1347–1365.
[35] F.S. Claudio, O. Gary, L. Nicolas, B. Michael, B. Carl, L. Marl, Discovery of a potent and selective prostaglandin D2 receptor antagonist, [(3R)-4-(4-chloro-benzyl)-7-fluoro-5-(methylsulfonyl)-1,2,3,4-tetrahydrocyclopent a[b]indol-3-yl]-acetic acid (MK-0524), J. Med. Chem 50 (2007) 794–806.
[36] X.F. Hu, Y.Q. Cao, X. Yin, L. Zhu, Y.Y. Chen, W.F. Wang, Design and synthesis of various quinizarin derivatives as potential anticancer agents in acute T lymphoblastic leukemia, Bioorg. Med. Chem. 27 (2019) 1262–1369.
[37] J. Craig, M.M. Elizabeth, R. Zoran, W. Grant, Medicinal chemistry of Herg optimizations: highlights and Hang-Ups, J. Med. Chem. 49 (2006) 5024–5029.
[38] H.J. Breslin, B.M. Lane, G.R. Ott, K.G. Arup, D.D. Bruce, Design, Synthesis, and Anaplastic Lymphoma Kinase (ALK) Inhibitory Activity for a Novel 2,4,8,22-Tetraazatetracyclo [14.3.1.1(3,7).1(9,13)]docosa-1(20),3(22),4,6,9(21),10,12,16,18 -nonaene Macrocycles, J. Med. Chem. 55 (2011) 449–464.
[39] D. Song, J.S. Yang, C. Oh, S. Cui, B.K. Kim, M. Won, J. Lee, H.M. Kim, G. Han, New synthetic aliphatic sulfonamide quaternary ammonium salts as anticancer chemotherapeutic agents, Eur. J. Med. Chem 69 (2013) 670–677.
[40] J.J. Lan, L. Huang, H.Y. Lou, C. Chen, T. Liu, S. Hu, Design and synthesis of novel C14-urea-tetrandrine derivatives with potent anticancer activity, Eur. J. Med. Chem. 143 (2018) 1968–1980.
[41] H. Zhou, X.M. Li, J. Meinkoth, Akt regulates cell survival and apoptosis at a postmitochondrial level, J. Cell Biol. 151 (2000) 483–494.
[42] J.F. Kerr, A.H. Wyllie, A.R. Currie, Apoptosis: a basic biological phenomenon with wide-ranging implications in tissue kinetics, Br. J. Cancer 26 (1972) 239–257.
[43] O. Tomoyo, S. Surajit, E. Ilaria, S. Gaia, L. Miguel, W.J. Su, The Rho GTPase Rnd1 suppresses mammary tumorigenesis and EMT by restraining ras-mapk signaling, Nat. Cell Biol. 17 (2015) 81–94.
[44] J. Rodon, R. Dienstmann, V. Serra, J. Tabernero, Development of PI3K inhibitors: Lessons learned from early clinical trials, Nat. Rev. Clin. Oncol. 10 (2013) 143–153.
[45] F. Wang, Q. Wang, Z.W. Zhou, S.N. Yu, S.T. Pan, Z.X. He, X.J. Zhang, D. Wang, Y. X. Yang, Plumbagin induces cell cycle arrest and autophagy and suppresses epithelial to mesenchymal transition involving PI3K/Akt/mTOR mediated pathway in human pancreatic cancer cells, Drug. Des. Dev. Ther. 9 (2015) 537–560.
[46] D. Aangelo, D. Noel, T.S. Kim, K. Andrews, S.K. Booker, Discovery and optimization of a series of benzothiazole phosphoinositide 3Kinase (PI3K)/ Mammalian target of rapamycin (mTOR)dual inhibitors, J. Med. Chem. 54 (2011) 1789–1812.
[47] H. Ma, J.Q. Zhu, Study on extraction process of alkaloids from Rhizoma chinensis and its antitumor activity, China Food 10 (2015) 66–68.